Biochimica et Biophysica Acta, 1023 (1990) 147–167
Elsevier

BBAMEM 74782

The binding of monoclonal and polyclonal antibodies to the Ca^{2+}-ATPase of sarcoplasmic reticulum: effects on interactions between ATPase molecules

Elek Molnar *, Norbert W. Seidler, Istvan Jona and Anthony N. Martonosi

Department of Biochemistry and Molecular Biology, State University of New York, Health Science Center at Syracuse, Syracuse, NY (U.S.A.)

(Received 6 October 1989)

Key words: ATPase, Ca^{2+}-; Antibody; Monoclonal antibody; Polyclonal antibody; ATPase–ATPase interaction; ATPase–antibody interaction; Sarcoplasmic reticulum

We analyzed the interaction of 14 monoclonal and 5 polyclonal anti-ATPase antibodies with the Ca^{2+}-ATPase of rabbit sarcoplasmic reticulum and correlated the location of their epitopes with their effects on ATPase–ATPase interactions and Ca^{2+} transport activity. All antibodies were found to bind with high affinity to the denatured Ca^{2+}-ATPase, but the binding to the native enzyme showed significant differences, depending on the location of antigenic sites within the ATPase molecule. Of the seven monoclonal antibodies directed against epitopes on the B tryptic fragment of the Ca^{2+}-ATPase, all except one (VIE8) reacted with the enzyme in native sarcoplasmic reticulum vesicles in both the E_1 and E_2V conformations. Therefore these regions of the Ca^{2+}-ATPase molecule are freely accessible in the native enzyme. The monoclonal antibody VIE8 bound with high affinity to the Ca^{2+}-ATPase only in the E_1 conformation stabilized by 0.5 mM Ca^{2+} but not in the E_2V conformation stabilized by 0.5 mM EGTA and 5 mM vanadate. Several antibodies that reacted with the B fragment interfered with the crystallization of Ca^{2+}-ATPase in the presence of EGTA and vanadate and at least two of them destabilized preformed Ca^{2+}-ATPase crystals, suggesting inhibition of interactions between ATPase molecules. Of five monoclonal antibodies with epitopes on the A_1 tryptic fragment of the Ca^{2+}-ATPase only one gave strong reaction with the native enzyme, and none interfered with ATPase–ATPase interactions as measured by the polarization of fluorescence of FITC-labeled Ca^{2+}-ATPase. Therefore the regions of the molecule containing these epitopes are relatively inaccessible in the native structure. Partial tryptic cleavage of the Ca^{2+}-ATPase into the A_1, A_2 and B fragments did not promote the reaction of anti-A_1 antibodies with sarcoplasmic reticulum vesicles, but solubilization of the membrane with $C_{12}E_8$ rendered the antigenic site fully accessible to several of them, suggesting that their epitopes are located in areas of contacts between ATPase molecules. Two monoclonal anti-B antibodies that interfered with ATPase–ATPase interactions, produced close to 50% inhibition of the rate of ATP-dependent Ca^{2+} transport, with significant inhibition of ATPase activity; this may suggest a role for ATPase oligomers in the regulation of Ca^{2+} transport. The other antibodies that interact with the native Ca^{2+}-ATPase produced no significant inhibition of ATPase activity even at saturating concentrations; therefore their antigenic sites do not undergo major movements during Ca^{2+} transport.

Introduction

About two-thirds of the mass of the Ca^{2+}-ATPase is exposed on the cytoplasmic surface of native sarcoplasmic reticulum; most of the remaining one-third is embedded into the lipid phase, and only small polypeptide segments may be exposed on the luminal side of the membrane [1–5].

The cytoplasmic domain of Ca^{2+}-ATPase contains the phosphate acceptor Asp-351 residue [6–8] and the binding site for ATP [9–11], while the residues involved in Ca^{2+} translocation are likely to be distributed in or near the transmembrane domain [12–15].

* On leave from the Institute of Biochemistry, Albert Szent-Gyorgyi University Medical School, H-6701 Szeged, Hungary.

Abbreviations: ELISA, enzyme-linked immunoadsorbent assay; SR, sarcoplasmic reticulum; Ca^{2+}-ATPase, the Ca^{2+},Mg^{2+}-activated ATPase of sarcoplasmic reticulum (EC 3.6.1.38); mAb, monoclonal antibody, pAb, polyclonal antibody; HRP, horseradish peroxidase; FITC, fluorescein 5′-isothiocyanate; IAEDANS, *N*-iodoacetyl-*N*′-(5-sulfo-1-naphthyl)ethylenediamine; AEDANS, IAEDANS covalently attached to the protein; $C_{12}E_8$, octaethyleneglycol dodecyl ether; AMP-PNP, 5′-adenylyl imidodiphosphate (p[NH]ppA).

Correspondence: A.N. Martonosi, Department of Biochemistry, SUNY, Health Science Center at Syracuse, Syracuse, NY 13210, U.S.A.

The location of functional sites on the Ca^{2+}-ATPase has been analyzed by fluorescent probes and by monoclonal and polyclonal antibodies.

The Ca^{2+}-ATPase can be selectively labeled with *N*-iodoacetyl-*N'*-(5-sulfo-1-naphthyl)ethylenediamine (IAEDANS) at Cys-670 and Cys-674 [16,17], and with fluorescein 5'-isothiocyanate (FITC) at Lys-515 [7,18], within the cytoplasmic domain. The distance between the AEDANS and FITC sites is 56 Å, based on fluorescenc resonance energy transfer measurements [19]. A similar distance of 68 Å was obtained between the covalently bound AEDANS and TNP-AMP presumed to be bound at the ATP binding site [19]. Competition between FITC and ATP for reaction with the Ca^{2+}-ATPase [20], places the FITC binding site (Lys-515) in the vicinity of the ATP binding domain. The 56–68 Å distance between the AEDANS and ATP binding sites roughly corresponds to the maximum dimension of the pear-shaped cytoplasmic domain of Ca^{2+}-ATPase, derived from electron microscope reconstructions of two-dimensional membrane crystals of the enzyme [2,3]. The distance between the calcium transport sites labeled with lanthanides and the binding sites for TNP-AMP or FITC was estimated to be 35 and 47 Å, respectively [12].

A wide selection of monoclonal and polyclonal antibodies with epitopes located on different regions of the Ca^{2+}-ATPase molecule have become available in recent years in various laboratories [21–51]. Most of these studies dealt with the cross-reactivity between Ca^{2+}-ATPase isoenzymes, their cellular localization and with the effects of antibodies on ATPase activity and Ca^{2+} transport. The localization of their epitopes within the ATPase contours defined by crystallography remains unknown.

The purpose of these studies was to obtain information on the accessibility of different regions of the Ca^{2+}-ATPase molecule to monoclonal and polyclonal antibodies of defined specificity and to relate the location of these antigenic sites to the effects of the antibodies on the ATPase–ATPase interactions and on the Ca^{2+} transport activity of sarcoplasmic reticulum.

Experimental Procedures

Materials

The sources of antibodies. Antibodies A22, A25, A52, E and N were provided by Dr. David H. MacLennan, Banting and Best Department of Medical Research, C.H. Best Institute, Faculty of Medicine, University of Toronto, Ontario, Canada M5G 1L6. Antibodies IIH11, $VE12_1G9$, VIE8 and IID8 were supplied by Dr. Kevin P. Campbell, Department of Physiology and Biophysics, University of Iowa, Iowa City, IA 52242, U.S.A. and antibodies 5C3, 5D2, 7C6, 4B4 and 8A6 by Dr. Douglas M. Fambrough, Department of Biology, Johns Hopkins University, Baltimore, MD 21218, U.S.A. Antibody D12 was from Dr. Angela F. Dulhunty, Department of Physiology and Experimental Pathology, John Curtin School of Medical Research, Australian National University, Canberra, A.C.T. 2601 Australia. Antibodies EM-1, EM-2 and EM-3 were prepared by Dr. Elek Molnar at the Institute of Biochemistry, Albert Szent-Gyorgyi University Medical School, H-6701 Szeged, Hungary.

Other chemicals. Disodium-ATP, EGTA, Tris, NADH, imidazole, phospho*enol*pyruvate, pyruvate kinase (rabbit muscle), lactate dehydrogenase (rabbit muscle), trypsin (bovine pancreas), trypsin inhibitor (soybean), acrylamide, bisacrylamide, ammonium persulfate, albumin (bovine serum), Tris-maleate, 4-chloro-1-naphthol, thimerosal, antifoam A concentrate, anti-rabbit, anti-sheep and anti-mouse IgG (whole molecule) peroxidase conjugates, polyoxyethylene sorbitan monolaurate (Tween 20), octaethyleneglycol dodecyl ether ($C_{12}E_8$), and *o*-phenylenediamine were supplied by Sigma Chemical Co., St. Louis, MO 63178, U.S.A. Sodium vanadate, potassium oxalate and 2-mercaptoethanol were purchased from Fisher Scientific Co., Fair Lawn, NJ 07410, U.S.A. Sodium dodecylsulfate was obtained from Polysciences, Inc., Washington, PA 18975, U.S.A.; *N,N,N',N'*-tetramethylethylenediamine (TEMED) from Eastman Organic Chemicals, Rochester, NY 14650, U.S.A.; Coomassie brilliant blue R-250, nitrocellulose sheets for Western blots and the ELISA plates were from Bio-Rad Laboratories, Richmond, CA 94804, U.S.A., and molecular weight markers from Pharmacia, Piscataway, NJ 08854, U.S.A. Fluorescein 5'-isothiocyanate was purchased from Molecular Probes, Inc., Eugene, OR 97402, U.S.A.; Ca^{2+} ionophore A23187 and Amido black 10-B was from Behring Diagnostics, La Jolla, CA 92037, U.S.A. Amersham Corporation provided $^{45}CaCl_2$. Rabbit anti-fluorescein antibody was supplied by Biomedical Technologies, Inc., Stoughton, MA 02072, U.S.A., and glycylglycine came from Aldrich Chemical Co., Milwaukee, WI 53233, U.S.A. All other chemicals were of analytical grade.

Methods

Isolation of sarcoplasmic reticulum. Sarcoplasmic reticulum (SR) vesicles were obtained by differential centrifugation of homogenates of predominantly white, rabbit skeletal muscle [52–54] and stored in 0.3 M sucrose and 10 mM Tris-maleate, pH 7.0 at −70 °C. Before assays, the sarcoplasmic reticulum vesicles were washed by centrifugation and resuspended in 0.1 M KCl, 10 mM imidazole (pH 7.4) and 5.0 mM $MgCl_2$. Protein was determined according to Lowry et al. [55].

Measurement of ATPase activity. The rate of Ca^{2+}-dependent ATP hydrolysis was determined by a coupled-enzyme system [54,56]. The assay was performed in a medium of 0.1 M KCl, 20 mM Tris-HCl (pH 7.5), 5 mM $MgCl_2$, ±0.5 mM $CaCl_2$, 0.5 mM EGTA, 5 mM

ATP, 0.2 mM NADH, 7.5 IU/ml pyruvate kinase, 18 IU/ml lactate dehydrogenase, 0.42 mM phospho*enol*-pyruvate and 1–2 μM A23187. Sarcoplasmic reticulum vesicles at a final concentration of 1–5 μg protein/ml were preincubated with various amounts of antibody, antiserum, preimmune serum, or buffer for 5 min at 24°C; the reaction was started with the addition of ATP-containing medium. The change in absorbance was measured at 340 nm at 24°C using a Perkin-Elmer Lambda 3B spectrophotometer. The Ca^{2+}-insensitive component of ATP hydrolysis was determined by omitting Ca^{2+} from the medium. Ca^{2+}-stimulated ATPase activity was obtained as the difference between the total and Ca^{2+}-insensitive rates of ATP hydrolysis. ATPase activities of the various antibody preparations were also measured in the absence of sarcoplasmic reticulum; some ascites fluid contained moderate ATPase activity and in these cases appropriate corrections were made to obtain the ATPase activity attributable to the Ca^{2+}-ATPase of sarcoplasmic reticulum.

Measurement of Ca^{2+} uptake. Ca^{2+} transport activity was determined by measuring the rate of ATP-dependent oxalate-potentiated uptake of $^{45}Ca^{2+}$ into sarcoplasmic reticulum vesicles. The final reaction mixture contained 0.1 M KCl, 10 mM imidazole (pH 7.4), 5 mM $MgCl_2$, 5 mM ATP, 10–100 μM $^{45}CaCl_2$ (0.02 μCi/ml) and 5 mM potassium oxalate. Sarcoplasmic reticulum vesicles (2–10 μg protein/ml) were preincubated in the presence of 0.1 M KCl, 10 mM imidazole (pH 7.4) and 5 mM $MgCl_2$ with various dilutions of antibody, antiserum, preimmune serum or buffer for 5–10 min at 20°C, before initiating the reaction by adding the Ca^{2+} uptake medium. Ca^{2+} uptake was followed at 20°C by filtering aliquots of the reaction mixture at intervals of 30 s through Millipore filters (0.45 μm pore size) for times ranging up to 5 min, as described by Martonosi and Feretos [57]. The rate of Ca^{2+} uptake was linear up to about 2 min of incubation time.

The preparation of polyclonal antibodies. For the preparation of antibodies against the rat skeletal muscle sarcoplasmic reticulum Ca^{2+}-ATPase, New Zealand rabbits were immunized with 2 mg sarcoplasmic reticulum Ca^{2+}-ATPase prepared from the gastrocnemius muscle of rats by the method of MacLennan [58]. For immunization the purified enzyme was suspended in complete Freund adjuvant and injected four times subcutaneously at 3-week intervals. The reactivity of the sera was tested using an ELISA method according to Goding [59]. The crossreaction with rabbit and fish sarcoplasmic reticulum Ca^{2+}-ATPase was established by immunoblotting [43]. The antisera were dialyzed at 4°C against 0.1 M KCl, 10 mM imidazole (pH 7.4), 5 mM $MgCl_2$ and 0.5 mM EGTA, before use in the experiments, to reduce the Ca^{2+} concentration.

Partial tryptic proteolysis of sarcoplasmic reticulum. The sarcoplasmic reticulum vesicles (2 mg protein/ml) were resuspended in 0.1 M KCl, 10 mM imidazole (pH 7.4), 5 mM $MgCl_2$ and 0.5 mM EGTA, and after preincubation for 5 min at 25°C, digestion was started with 0.05 mg trypsin/ml (25 μg trypsin/mg sarcoplasmic reticulum protein) at 25°C for 15 min, as described earlier [60]. The digestion was stopped with 0.2 mg soybean trypsin inhibitor/ml of solution, and the samples were processed for SDS-polyacrylamide gel electrophoresis in 6–18% gradient gels, essentially according to Laemmli [61]. Control samples, without trypsin and trypsin inhibitor, were included in each experiment.

Labeling of Ca^{2+}-ATPase with fluorescein 5′-isothiocyanate (FITC). Sarcoplasmic reticulum vesicles (2 mg protein/ml) suspended in 0.3 M sucrose, 50 mM Tris-HCl (pH 8.0), 5 mM $MgCl_2$, 0.1 mM EGTA, were reacted with 5 nmol FITC/mg SR protein, at 25°C for 30 min in the dark. After labeling the samples were diluted 10-fold with 20 mM K-Mops (pH 7) and centrifuged at 2°C at 49000 × *g* for 40 min to remove the unreacted dye; the sedimented vesicles were resuspended in 0.1 M KCl, 10 mM imidazole (pH 7.4) and 5 mM $MgCl_2$.

For electrophoresis on sodium dodecylsulfate-polyacrylamide gradient (6–18%) gels [61], the samples were dissolved in a solution of 5% sodium dodecylsulfate, 10 mM Tris-HCl (pH 8.0), 1% β-mercaptoethanol, 10% glycerol, and 0.05% Bromophenol blue; after incubation for 5 min at 100°C, aliquots containing 30 μg protein were applied to the gels. Phosphorylase *b* (94 kDa), bovine serum albumin (67 kDa), ovalbumin (43 kDa), carbonic anhydrase (30 kDa), soybean trypsin inhibitor (20 kDa) and α-lactalbumin (14.4 kDa) were used as molecular weight markers (Pharmacia, Piscataway, NJ 08854, U.S.A.).

Electrophoretic transfer for immunoblot analysis of sarcoplasmic reticulum proteins. After SDS-polyacrylamide gel electrophoresis, the proteins were transferred to nitrocellulose sheets (Bio-Rad 14 × 18 cm, 0.45 μm pore size) using an LKB Transphor-electroblotting unit. The transfer buffer contained 10 mM imidazole, 30 mM glycylglycine, 0.1% sodium dodecylsulfate, and 20% methanol (pH 8.3). The transfer required 3 h at 40 V, and a temperature of 10–15°C.

For localization of proteins the nitrocellulose sheets were stained with 0.2% (w/v) Amido black for 5 min in 45% methanol, 10% acetic acid solution and then destained in 25% methanol, 5% acetic acid.

Immunostaining of nitrocellulose membranes. After the electrophoretic transfer, the nitrocellulose sheets were immersed in a solution of 5% (w/v) nonfat dry milk, 0.01% Antifoam A, and 0.0001% merthiolate in a phosphate-buffered saline (PBS) solution containing 1.5 mM KH_2PO_4, 8.1 mM Na_2HPO_4 (pH 7.2), 0.137 M NaCl and 2.7 mM KCl, for 2 h [62]. The sheets were then

incubated for 2 h with a 1 : 1000 dilution of the various antisera in phosphate-buffered saline, containing 1% milk powder at room temperature. After washing twice for 5 min with phosphate-buffered saline containing 0.05% Tween 20, and once with phosphate-buffered saline containing 1% milk powder, the membrane filters were incubated for 2 h at room temperature with horseradish-peroxidase conjugated anti-mouse, anti-sheep or anti-rabbit IgG (Sigma Chemical Co., St. Louis, MO 63178, U.S.A.), diluted to 1 : 1000 in phosphate-buffered saline containing 1% milk powder. The reaction was terminated by washing the sheets twice for 5 min each with phosphate-buffered saline containing 0.05% Tween 20 and once with a solution of 0.9% NaCl and 10 mM Tris (pH 7.4). The bound, conjugated IgG was visualized by reaction for ≅ 15 min with a solution containing 10 ml 0.9% NaCl, 10 mM Tris (pH 7.4), 1 ml of 0.3% 4-chloro-1-naphthol in methanol and 0.01 ml of 30% (v/v) H_2O_2. When bands became visible, the nitrocellulose filters were rinsed with distilled water, photographed and dried at room temperature for subsequent analysis.

Enzyme-linked immunoadsorbent assay (ELISA). Sarcoplasmic reticulum proteins (0.03, 0.1, 0.3 and 1 μg) were dispersed in 100 μl coating buffer (13 mM sodium carbonate, 35 mM sodium bicarbonate, pH 9.6) and immobilized in polyvinyl chloride microtiter wells (Bio-Rad), at 4° C for 12 h. The plates were washed three times for 3 min each with washing buffer containing 0.05% Tween 20 in phosphate-buffered saline (PBS) (pH 7.2). 100-μl aliquots of 1% solution of bovine serum albumin in PBS were added to each well and incubated for 1 h at room temperature. The plates were then reacted with a 1 : 1000 dilution of the antibody for 1 h at room temperature, followed by washing the wells with the washing buffer. The bound antibody was reacted with horseradish peroxidase conjugates of anti-mouse, anti-rabbit or anti-sheep antibodies (1 : 1000 dilution) for 1 hour at room temperature. Finally, the plates were rinsed and reacted for 30 min with a substrate solution of 67 mM sodium dibasic phosphate, 35 mM citric acid (pH 5.0), 0.08% *o*-phenylenediamine and 0.03% H_2O_2, to form a colored product for spectroscopy. The reaction was terminated with 50 μl of 2 M sulfuric acid, and the absorbance was determined at 405 nm with a Titertek Multiskan microtitration plate photometer (No. 78504) produced by Flow Laboratories, Inc., McLean, VA 22102, U.S.A.

The amount of fixed antigen on the ELISA plates (Bio-Rad) was determined by the malachite green modification of the Lowry protein assay, as described by Sargent [63]. The modified Lowry assay was performed in the wells of the ELISA plate in a final volume of 220 μl; the absorbance was measured at 700 nm with a Titertek Multiskan microtitration plate photometer (Flow Laboratories, Inc.).

Crystallization of Ca^{2+}-ATPase and electron microscopy. A stock suspension of sarcoplasmic reticulum vesicles (≅ 35 mg protein/ml) was washed by centrifugation and resuspended in 0.1 M KCl, 10 mM imidazole (pH 7.4), and 10 mg protein/ml just prior to the experiments. The standard crystallization medium consisted of 0.1 M KCl, 10 mM imidazole (pH 7.4), 5 mM $MgCl_2$, 0.5 mM EGTA and 5 mM Na_3VO_4. Sarcoplasmic reticulum protein concentration was 0.67–1 mg/ml. The formation of two-dimensional Ca^{2+}-ATPase crystals at 2° C can be seen within a few hours and becomes quite extensive after 24 h [64–67].

Antibody preparations were added either before or after crystallization of Ca^{2+}-ATPase. When added before crystallization, antibodies at several concentrations were incubated at 2–4° C with sarcoplasmic reticulum vesicles for various times in 0.1 M KCl, 10 mM imidazole (pH 7.4) and 5.0 mM $MgCl_2$ prior to addition of standard crystallization medium. The crystallization was allowed to proceed for a 24 h period, and aliquots were taken for electron microscopy. Alternatively, Ca^{2+}-ATPase crystals were first induced by overnight incubation at 2–4° C in the vanadate-containing crystallization medium prior to adding varying amounts of antibody. Aliquots were removed for electron microscopy on the following day.

For electron microscopy, a small volume of the incubation mixture was deposited on a carbon-coated parlodion film, and negatively stained with 1% uranyl acetate, pH 4.3 at 4° C. The samples were viewed in a Siemens Elmiskop I microscope at 60 kV.

Results

The monoclonal and polyclonal antibodies used in these studies are listed in Table I, together with information about their specificity, and host species. Previous reports on monoclonal antibodies A25, A22, and A52 established their specificity with respect to isoenzymes of Ca^{2+}-ATPase obtained from different types of muscles of various species [33,34]. Based on personal communication from Dr. D.H. MacLennan, the epitope for A25 is located in the sequence region 328–505, that for A22 in 506–738, and that for A52 in 659–668 of the Ca^{2+}-ATPase. Monoclonal antibody D12 was used by Dulhunty et al. [40], for quantitative immunohistochemical analysis of Ca^{2+}-ATPase distribution in slow-twitch and fast-twitch skeletal muscles of rabbit, rat and toad. Immunohistochemical localization and cross-reaction of Ca^{2+}-ATPase isoenzymes from dog cardiac and skeletal muscles with antibodies IID8 and IIH11 was reported by Jørgensen et al. [28]. Antibodies 5C3, 5D2, 7C6, 4B4, 8A6 and 11A4 were analyzed for isoenzyme and species specificity by Karin et al. [50]. Polyclonal antibodies EM-1, EM-2 and EM-3 were raised against Ca^{2+}-ATPase from rat skeletal muscle

TABLE I

Characteristics of the antibodies

Antibodies A22, A25, A52, E and N were provided by Dr. David H. MacLennan, Banting and Best Dept. of Medical Research, C.H. Best Institute, Faculty of Medicine, University of Toronto, Ontario, Canada M5G 1L6; antibodies IIH11, VE12,$_1$G9, VIE8 and IID8 by Dr. Kevin P. Campbell, Dept. of Physiology and Biophysics, University of Iowa, Iowa City, IA 52242, U.S.A.; and antibodies 5C3, 5D2, 7C6, 4B4 and 8A6 by Dr. Douglas M. Fambrough, Dept. of Biology, Johns Hopkins University, Baltimore, MD 21218, U.S.A. Antibody D12 was obtained from Dr. Angela F. Dulhunty, Dept. of Physiology and Experimental Pathology, John Curtin School of Medical Research, Australian National University, Canberra, A.C.T. 2601, Australia. Antibodies EM-1, EM-2 and EM-2 were prepared by Dr. Elek Molnar at the Institute of Biochemistry, Albert Szent-Gyorgyi University Medical School, Szeged, Hungary. For other details, see text. SSR, skeletal muscle sarcoplasmic reticulum; CSR, cardiac sarcoplasmic reticulum; f Ca^{2+}-ATPase, the fast isoenzyme of Ca^{2+}-ATPase, p, purified IgG or IgM; a, ascites fluid without further purification.

Antibody		Antigen		Host species	Preparation	[Protein] (mg/ml)	Antigen locus			Inhibition of crystallization
code	type	species	enzyme				tryptic fragment	sequence	exposed in native SR	
A25	mono	rabbit	SSR	mouse	IgG(p)	1.0	A_1	328–505	–	–
IIH11	mono	rabbit	f Ca^2-ATPase	mouse	IgG(a)	30.4	A_1		–	–
7C6	mono	rabbit	f Ca^2-ATPase	mouse	IgG(p)	2.4	A_1		+	–
8A6	mono	rabbit	f Ca^2-ATPase	mouse	IgG(p)	3.9	A_1		–	–
11A4	mono	rabbit	f Ca^2-ATPase	mouse	IgG(p)	3.9	A_1		–	–
A22	mono	rabbit	f Ca^2-ATPase	mouse	IgM(p)	4.0	B	506-738	+	–
A52	mono	rabbit	f Ca^2-ATPase	mouse	IgG(p)	2.0	B	659-668	+	+
VE12$_1$G9	mono	rabbit	f Ca^2-ATPase	mouse	IgG(a)	30.1	B		+	+
VIE8	mono	rabbit	f Ca^2-ATPase	mouse	IgG(a)	19.5	B		+[a]	–
5D2	mono	rabbit	f Ca^2-ATPase	mouse	IgG(p)	1.3	B		+	–
4B4	mono	rabbit	f Ca^2-ATPase	mouse	IgG(p)	5.9	B		+	+
D12	mono	rabbit	f Ca^2-ATPase	mouse	IgG(p)	2.0	B		+	+
E	poly	rabbit	f Ca^2-ATPase	sheep	IgG(p)	5.0	A_2+A_1+B		+	+
N	poly	rabbit	f Ca^2-ATPase	rabbit	serum	72.0	A_2+A_1+B		+	+
EM-1	poly	rat	f Ca^2-ATPase	rabbit	serum	46.0	A_2+B		+	–
EM-2	poly	rat	f Ca^2-ATPase	rabbit	serum	63.0	A_2+A_1+B		+	–
EM-3	poly	rat	f Ca^2-ATPase	rabbit	serum	73.0	A_2+A_1+B		+	–
IID8	mono	dog	CSR Ca^{2+}-ATPase	mouse	IgG(a)	23.0				
5C3	mono	chicken	SSR Ca^{2+}-ATPase	mouse	IgG(p)	2.0				

[a] Binding was observed only in the E_1 but not in the E_2V conformation.

and tested for cross-reaction with rabbit and carp skeletal and rat cardiac muscle sarcoplasmic reticulum by Sarkadi et al. [43] and Krenacs et al. [45].

The antigenic determinants of the monoclonal and polyclonal anti-ATPase antibodies (Table I) were localized in the structure of Ca^{2+}-ATPase by analyzing their reaction with the tryptic fragments of the enzyme produced by partial proteolysis (Fig 1).

Tryptic cleavage at the T_1 bond, located between residues 505 and 506, yields an N-terminal A fragment of 57 kDa and a C-terminal B fragment of 52 kDa, that migrate close to each other on SDS-polyacrylamide gels [68]. The B fragment can be selectively labeled by fluorescein 5′-isothiocyanate [18] and visualized by its fluorescence emission. Secondary cleavage of the A fragment at the T_2 cleavage site between residues 198 and 199 produces the A_2 fragment of 23 kDa, that retains the N-terminal segment of the intact ATPase, and an A_1 fragment of 34 kDa that contains the phosphate acceptor aspartyl group at position 351. The cleavage of the Ca^{2+}-ATPase at the T_2 site can be completely blocked by vanadate in the presence of EGTA, without effect on the T_1 cleavage [60,65,69], permitting the production of A and B fragments from the Ca^{2+}-ATPase in good yield, uncomplicated by hydrolysis at secondary sites.

All antibodies raised against Ca^{2+}-ATPase from rabbit and rat sarcoplasmic reticulum reacted specifically with the Ca^{2+}-ATPase after denaturation in sodium dodecylsulfate and separation by SDS-polyacrylamide gel electrophoresis. Monoclonal antibody IID8 against dog cardiac Ca^{2+}-ATPase and 5C3 against chicken skeletal muscle Ca^{2+}-ATPase did not react with Ca^{2+}-ATPase from rabbit fast-twitch skeletal muscle.

For localization of the antigenic determinants in the various ATPase fragments, the intact Ca^{2+}-ATPase and its tryptic fragments were separated by SDS-polyacrylamide gel electrophoresis, transferred onto nitrocellulose sheets and reacted with antibodies. The protein bound antibody was coupled with horseradish peroxidase conjugated anti-host IgG, and visualized by reacting with the horseradish peroxidase substrates *o*-phenylenediamine and H_2O_2.

As shown in Fig. 1A, the monoclonal antibodies

A25, IIH11, 7C6, 8A6 and 11A4 reacted with the A and the A_1 fragments of the Ca^{2+}-ATPase, indicating that their antigenic determinants are located between amino acid residues 199 and 505. Therefore these antibodies are described as anti-A_1 antibodies. The binding of A25 to the A_1 fragment was earlier observed by Zubrzycka-

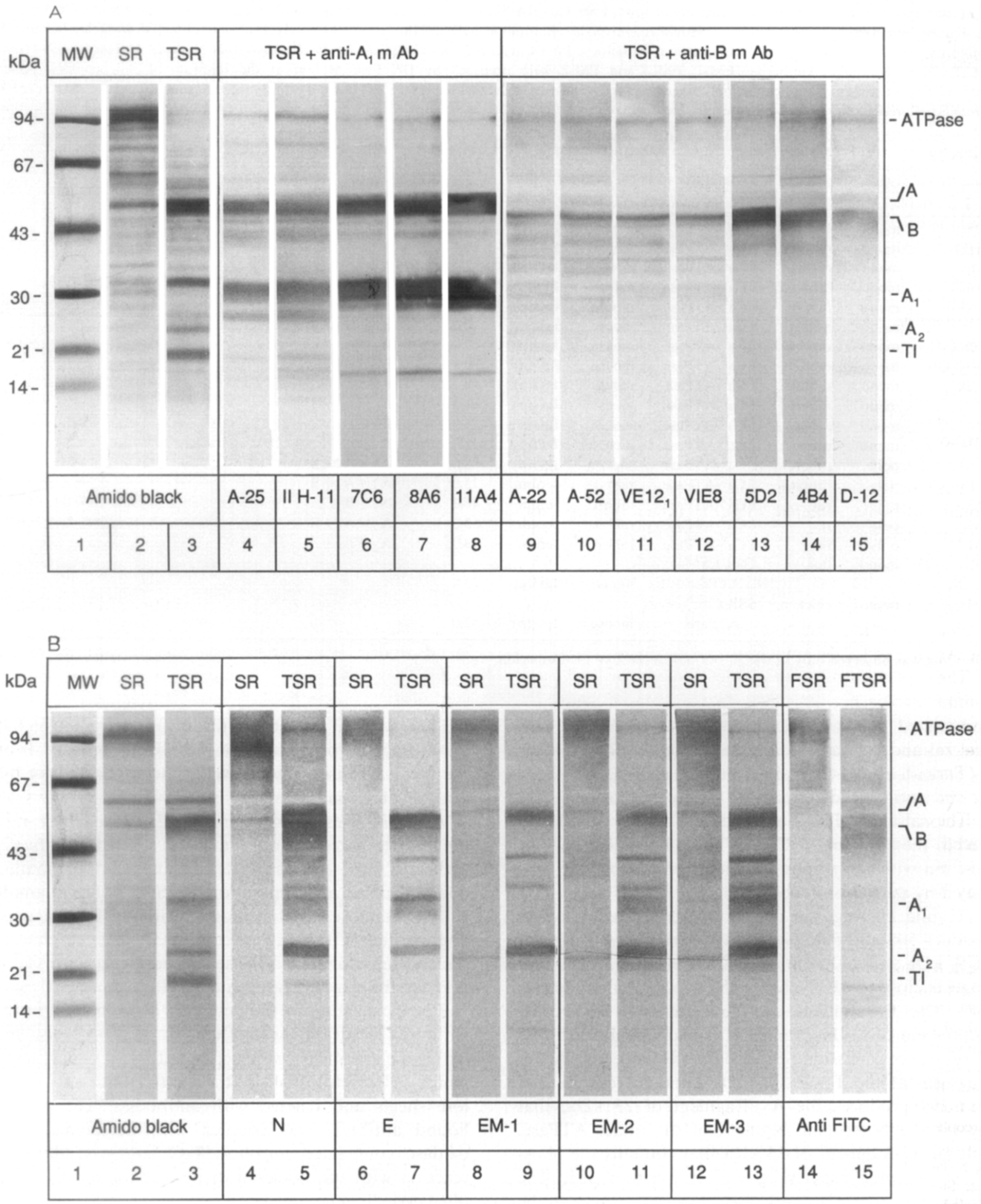

Gaarn et al. [34] and its epitope resides between residues 328 and 505 (MacLennan, D.H., personal communication).

Monoclonal antibodies A22, A52, $VE12_1G9$, VIE8, 5D2, 4B4 and D12 react exclusively with the B fragment of the Ca^{2+}-ATPase (Fig. 1A). In agreement with these observations, the antigenic determinants of antibodies A22 and A52 were assigned to the regions between residues 506–738 and residues 659–668, respectively (MacLennan, D.H., personal communication). Antibodies A22, A52, $VE12_1G9$, VIE8, 5D2, 4B4 and D12 are collectively described as anti-B antibodies. The anti-FITC antibody prepared in rabbits against FITC-labeled keyhole limpet hemocyanine also reacts, as expected, with the B fragment covalently labeled with FITC at lysine 515 (Fig. 1B).

Curiously, so far we have not found a monoclonal antibody with an antigenic determinant in the A_2 fragment of the Ca^{2+}-ATPase. Therefore the A_2 region may remain folded or obstructed by aggregation during immunization. Similar observation was reported recently by Colyer et al. [51] with a different set of monoclonal antibodies.

As expected, the reaction pattern of polyclonal anti-ATPase antibodies is more complex (Fig. 1B). All polyclonal antibodies reacted with the intact ATPase and with the tryptic B fragment, but in addition, antibody EM-1 also reacted with the A_2 fragment and antibodies E, N, EM-2 and EM-3 with the A_1 and A_2 fragments. Other bands indicate reaction of antibodies with minor cleavage products due to continued slow hydrolysis of the A_1, A_2 and B fragments.

The reaction pattern of the various antibodies is summarized in Fig. 2.

The reaction of anti-ATPase antibodies with the Ca^{2+}-ATPase in the E_1 and E_2V conformation in native sarcoplasmic reticulum vesicles

The monoclonal and polyclonal antibodies are produced against denatured Ca^{2+}-ATPase. Since denaturation presumably unfolds the molecule, antigenic sites may become exposed that are not readily accessible in the native enzyme [70]. The accessibility of the antigenic determinants in the native Ca^{2+}-ATPase was investigated by measuring the antigen binding capacity of the various antibody preparations before and after incubation with native sarcoplasmic reticulum vesicles in the E_1 and E_2V state using a quantitative ELISA technique.

Various dilutions of antibody solutions (1 : 5, 1 : 20, 1 : 100) were preincubated with sarcoplasmic reticulum vesicles (0.67 mg protein/ml) either in a medium containing 0.1M KCl, 10 mM imidazole (pH 7.4), 5 mM $MgCl_2$ and 0.5 mM $CaCl_2$ (E_1 state), or in a medium of 0.1 M KCl, 10 mM imidazole (pH 7.4), 5 mM $MgCl_2$, 0.5 mM EGTA and 5 mM sodium vanadate (E_2V state).

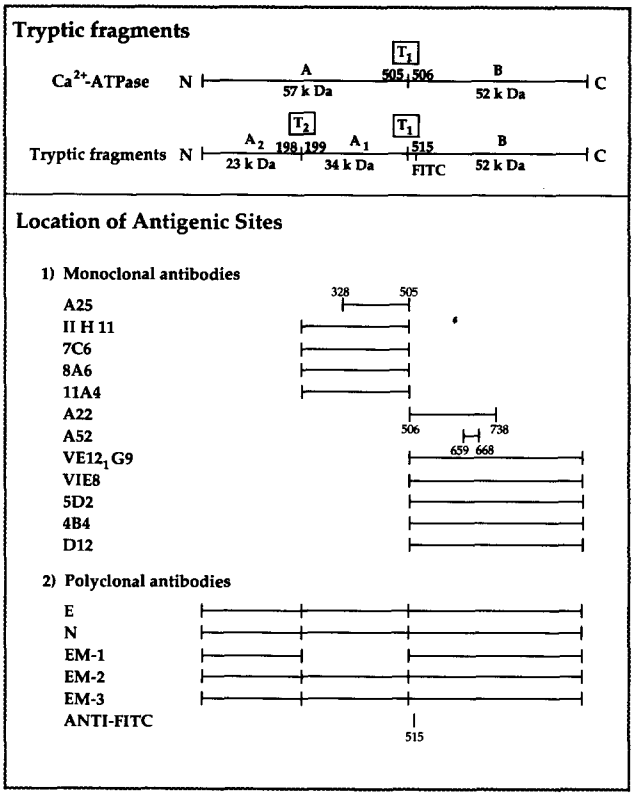

Fig. 2. Scheme of the distribution of antigenic sites for the various antibodies in the tryptic fragments of the Ca^{2+}-ATPase. For details, see text.

Fig. 1. Reaction of antibodies with the tryptic fragments of the Ca^{2+}-ATPase. Sarcoplasmic reticulum proteins were partially digested with trypsin (25 μg trypsin/mg SR protein, 15 minutes at 25° C) to yield the A, A_1, A_2 and B tryptic fragments, as described in Methods. The products of proteolysis were separated by SDS-polyacrylamide gel electrophoresis on 6–18% gradient gels [61], transferred to nitrocellulose sheets, and either stained with Amido black or incubated with 1 : 1000 dilution of the various antibodies, as described under Methods. Each sample contained the equivalent of 30 μg of sarcoplasmic reticulum protein. The bound antibodies were detected by reaction with horseradish peroxidase-conjugated anti-host IgG antibody. (A) Monoclonal antibodies. Lane 1, molecular weight markers; lane 2, sarcoplasmic reticulum proteins stained with Amido black; lane 3, trypsin cleaved sarcoplasmic reticulum proteins, stained with Amido black. Lanes 4–15, the monoclonal antibodies used for reaction are from left to right as follows: A25, IIH11, 7C6, 8A6, 11A4, A22, A52, $VE12_1G9$, VIE8, 5D2, 4B4 and D12; the antigen in each case was sarcoplasmic reticulum digested with trypsin, as described above. (B) Polyclonal antibodies. Lane 1, molecular weight markers. Lanes 2 and 3 contain native and trypsin-cleaved sarcoplasmic reticulum, stained with Amido black. In lanes 4–15 the polyclonal antibodies used were N (lanes 4, 5), E (lanes 6, 7), EM-1 (lanes 8, 9), EM-2 (lanes 10, 11), EM-3 (lanes 12, 13), and an anti-FITC antibody supplied by Biomedical Technologies, Inc., Stoughton, MA 02072, U.S.A. (lanes 14, 15). The Ca^{2+}-ATPase used as antigen with the anti-FITC antibody in lanes 14, 15 was covalently labeled with FITC, as described under Experimental Procedures. In lanes 2, 4, 6, 8, 10, 12 and 14 the antigen was undigested sarcoplasmic reticulum, while in lanes 3, 5, 7, 9, 11, 13 and 15 sarcoplasmic reticulum was previously digested with trypsin as described above.

Control antibody solutions were incubated under the same conditions without sarcoplasmic reticulum. After preincubation both solutions were centrifuged at 10000 $\times g$ for 1 h and the supernatants containing the unbound antibody were analyzed by ELISA.

(a) Anti-A_1 antibodies. Preincubation with native sarcoplasmic reticulum in the E_1 or E_2V states had no measurable influence on the antigen binding capacity of supernatant solutions in the case of monoclonal antibodies A25, IIH11, 8A6 and 11A4 even at 1 : 100 dilution where the assay is most sensitive (Fig. 3, Table II); therefore these antibodies did not interact significantly with their antigenic determinants in the native sarcoplasmic reticulum. Of the five anti-A_1 antibodies that were tested, only mAb 7C6 reacted significantly with the Ca^{2+}-ATPase in native sarcoplasmic reticulum, as indicated by the diminished ELISA reaction in the supernatant solution after preincubation with 0.67 mg sarcoplasmic reticulum protein/ml (Fig. 3, Table II). The binding of mAb 7C6 to the Ca^{2+}-ATPase was similar in the E_1 and E_2V states (Table II).

The binding capacity of the anti A_1 antibodies A25, IIH11, 8A6 and IIA4 to the tryptic fragments of the Ca^{2+}-ATPase was tested by competitive ELISA, essentially as described in Figs. 3–4, except that the preincubation of antibodies was performed with sarcoplasmic reticulum vesicles that were previously digested with trypsin. The digestion was done either in the presence of 0.1 mM Ca^{2+} that resulted in cleavage at the T_1 and T_2 sites, or in the presence of 0.5 mM EGTA and 5mM vanadate, where the cleavage was restricted to the T_1 site. Even after tryptic hydrolysis under either conditions, the antigenic sites of the Ca^{2+}-ATPase remained inaccessible to all four anti-A_1 antibodies that were tested. This is not surprising in view of the retention of ATPase activity and conformational responses of the Ca^{2+}-ATPase after partial proteolysis [60].

(b) Anti-B antibodies. In striking contrast to the inaccessibility of antigenic sites in the A_1 region, most of the anti-B antibodies reacted significantly with their antigenic determinants in the E_1 and E_2V states in the native Ca^{2+}-ATPase (Fig. 4, Table II). Preincubation with native sarcoplasmic reticulum produced large depletion of the free antibody concentration of the supernatant solution in the case of mAb A22, A52, 4B4, 5D2, $VE12_1G9$ and D12 at 1 : 100 dilution (Fig. 4, Table II); significant binding to the Ca^{2+}-ATPase was detected with antibody A22 even at 1 : 5 dilution, and with A52 at 1 : 20 dilution. It appears from these data that the antigenic sites are more accessible to antibodies in the region of the native Ca^{2+}-ATPase molecule corresponding to the tryptic B fragment, than in the region of the A_1 fragment.

One of the anti-B monoclonal antibodies, VIE8, did not react significantly with the Ca^{2+}-ATPase in the native sarcoplasmic reticulum vesicles in the E_2V state, although it had relatively high affinity for the Ca^{2+}-ATPase in the native E_1 state or after adsorption to plastic in the solid-phase immunoassay (Fig. 4, Table II). Therefore the epitope of VIE8 may either undergo structural change in the E_2V state, causing the loss of its antigenic character, or becomes occluded.

(c) Polyclonal antibodies. All polyclonal antibodies (E, N, EM-1, EM-2, EM-3) and the anti-FITC antibody reacted freely with the Ca^{2+}-ATPase in native sarcoplasmic reticulum in both E_1 and E_2V conformations, as indicated by the depletion of the free antibody con-

TABLE II

The binding of antibodies to the Ca^{2+}-ATPase in the E_1 and E_2V conformations

Antibody solutions diluted 1 : 100 were preincubated at 2°C with sarcoplasmic reticulum (0.67 mg protein/ml) or without sarcoplasmic reticulum, in a medium of 0.1 M KCl, 10 mM imidazole (pH 7.4) and 5 mM $MgCl_2$ and 0.5 mM $CaCl_2$ (E_1 state), or in a medium of 0.1 M KCl, 10 mM imidazole (pH 7.4), 5 mM $MgCl_2$, 0.5 mM EGTA and 5 mM Na_3VO_4 (E_2V) state, essentially as described in the legend to Figs. 3 and 4. The concentration of free antibody was determined after centrifugation at 10000 $\times g$ for 1 h by analysis of the supernatant with ELISA, using 1 μg sarcoplasmic reticulum protein fixed to the wells of the microtiter plates. Control antibody solutions were subjected to the same procedure except that sarcoplasmic reticulum was omitted during preincubation. The absorbance of the products of peroxidase reaction was measured at 405 nm, using a Titertek microtitration plate photometer. The difference in absorbance between the control samples and the samples obtained after preincubation with the sarcoplasmic reticulum was expressed as percent of the control absorbance to illustrate the antibody binding to the native sarcoplasmic reticulum. Column 1 identifies the code name of the antibody and column 2 the location of the epitopes in the various tryptic fragments of the Ca^{2+}-ATPase.

Antibody	Epitope	Fraction of Ab bound to native sarcoplasmic reticulum (%)	
		E_1	E_2
A25	A_1	0	0
IIH11	A_1	0	0
7C6	A_1	71	48
8A6	A_1	0	0
11A4	A_1	0	0
A22	B	100	100
A52	B	75	76
$VE12_1G9$	B	38	38
VIE8	B	39	0
5D2	B	80	59
4B4	B	41	67
D12	B	90	71
E	A_1 A_2 B	33	23
N	A_1 A_2 B	90	62
EM-1	A_2 B	34	35
EM-2	A_1 A_2 B	14	32
EM-3	A_1 A_2 B	21	19
IID8	–	0	0
5C3	–	0	0
Anti-FITC	B	68	75

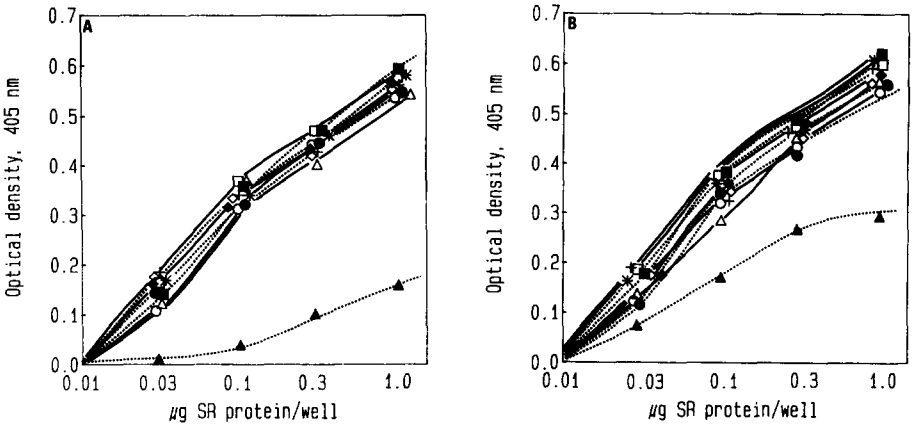

Fig. 3. Symbols: mAb A25 (○, ●); IIH11 (□, ■); 7C6 (△, ▲); 8A6 (+, *); and 11A4 (◇, ◆).

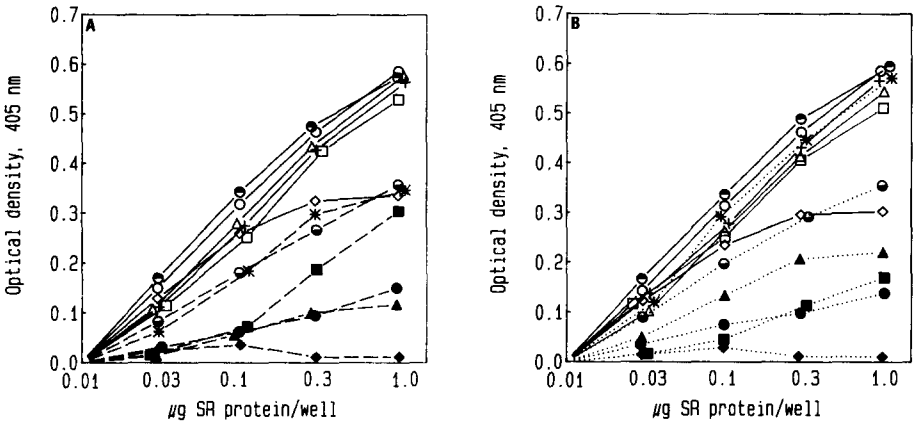

Fig. 4. Symbols: mAb A22 (◇, ◆), A52 (○, ●); VE12$_1$G9 (⊖, ⊖); VIE8 (+, *); 5D2 (△, ▲) and 4B4 (◇, ◆).

Fig. 3 and 4. Determination of antibody binding to Ca^{2+}-ATPase in native sarcoplasmic reticulum in the E_1 and E_2V states by enzyme-linked immunoadsorbent (ELISA) assay. Sarcoplasmic reticulum vesicles (0.67 mg/ml) were preincubated with the various antobidies at 1:100 dilution for 2 hours at 2°C, in a medium containing 0.1 M KCl, 10 mM imidazole (pH 7.4), 5 mM $MgCl_2$, and either 0.5 mM $CaCl_2$ (Figs. 3A and 4A, E_1 state), or 0.5 mM EGTA and 5 mM Na_3VO_4 (Figs. 3B and 4B, E_2V state) (●, ■, ▲, *, ◆, ⊖; broken lines). In a parallel series of control experiments the antibodies were incubated under identical conditions in the absence of sarcoplasmic reticulum (○, □, △, +, ◇, ⊖; solid lines). The unbound antibody in the medium was determined by centrifuging the samples at 10000 × *g* for 1 h and analyzing the supernatant solutions by ELISA at a 1:10 dilution (total dilution of Ab 1:1000), as described under Methods, using sarcoplasmic reticulum vesicles adsorbed to plastic in amounts of 0, 0.03, 0.1, 0.3 and 1 μg per well. The absorbance of the products of peroxidase reaction was determined at 405 nm, using a Titertek Multiskan microtitration plate photometer (Flow Laboratories, Inc.). The absorbance at 405 nm is plotted versus the concentration of antigen expressed as μg protein/well.

centration after preincubation of immune sera at 100-fold dilution with sarcoplasmic reticulum vesicles (Table II). In most cases significant binding was observed at 5–20-fold antibody dilutions as well. The reactivity of polyclonal antibodies with the native Ca^{2+}-ATPase is probably related to the presence of epitopes in the region of the B fragment, although these antibodies have antigenic sites in the A fragment as well.

Unmasking of the antigenic sites

The hidden antigenic site of the A25 anti-A_1 antibody can be exposed by solubilization of the sarcoplasmic reticulum with the neutral detergent $C_{12}E_8$ (Table III). The subsequent ELISA test of the supernatant indicates that at an antibody dilution of 1:100 more than 90% of the A25 antibody was bound to the Ca^{2+}-ATPase in the presence of 4 mg $C_{12}E_8$/mg sarcoplasmic reticulum protein, while in the absence of $C_{12}E_8$ essentially no binding could be observed. The binding of antibody 8A6 was also promoted by $C_{12}E_8$, while under the same conditions there was only slight binding of IIH11 or 11A4 (Table III). Deoxycholate (0.7–1.0 mg/ml) increased the binding of 8A6 and 11A4 but had no effect on IIH11 (Table III). These observations imply either some unfolding of the protein in detergent solutions, or that antigenic sites blocked by interactions between ATPase molecules in the native membrane become exposed in detergent solutions, due to dissocia-

TABLE III

Effect of $C_{12}E_8$ on the binding of monoclonal antibodies to the Ca^{2+}-ATPase

Sarcoplasmic reticulum was solubilized with $C_{12}E_8$ or deoxycholate (DOC) at varying detergent/protein ratios. The detergent-treated sarcoplasmic reticulum (0.67 mg protein/ml) was preincubated with monoclonal antibodies A25, IIH11, 8A6 and 11A4 at 1:100 dilution at 2°C overnight, followed by centrifugation at 10000×*g* for 1 h. The supernatant was tested at 1:10 dilution for antibody reaction on ELISA plates containing 1 μg sarcoplasmic reticulum protein per well. Antibody solutions without $C_{12}E_8$ and with 2.68 mg $C_{12}E_8$/ml were used as control. The reaction obtained in the control samples (100%) served as a reference for samples preincubated with sarcoplasmic reticulum in the presence of $C_{12}E_8$. After 1 h incubation the binding of antibody 8A6 in the presence of 4 mg $C_{12}E_8$ per mg protein was less than 10% of control in media containing 0.5 mM EGTA or 0.01–10 mM Ca^{2+}; therefore even in the presence of detergents the binding of 8A6 to the Ca^{2+}-ATPase is a relatively slow process.

Detergent		Antibody bound (% of control)			
mg/ml	mg/mg protein	A25	IIH11	8A6	11A4
$C_{12}E_8$					
0	0.0	0	0	0	0
0.26	0.4	58	0	11	0
0.52	0.8	71	2	9	0
1.34	2.0	81	4	31	0
2.68	4.0	92	3	42	8
DOC					
0	0.0	–	0	0	2
0.13	0.2	–	5	19	1
0.47	0.7	–	1	55	50
0.67	1.0	–	5	75	65

tion of ATPase oligomers. The epitope of IIH11 is apparently exposed only after complete denaturation of the enzyme. Similar changes may explain the fact that all antibodies used in these studies react with the denatured Ca^{2+}-ATPase adsorbed on ELISA wells or separated on SDS-polyacrylamide gels.

Exposure of sarcoplasmic reticulum vesicles to 1.5 kbar pressure for 2 h at 21°C inhibits the Ca^{2+} transport activity [54] and produces structural changes in the Ca^{2+}-ATPase visible by Fourier transform infrared spectroscopy. Vanadate in a Ca^{2+}-free medium protects the Ca^{2+}-ATPase against inactivation by high pressure [54]. Pressure treatment (1.5 kbar for 2 h) exposed the antigenic sites for 8A6 and 11A4 with or without EGTA (0.5 mM), vanadate (5 mM) or Ca^{2+} (20 mM) in the incubation medium, but had no significant effect on the reaction of IIH11 with the Ca^{2+}-ATPase.

Effect of antibodies on the stability of Ca^{2+}-ATPase crystals

The reconstruction of the structure of Ca^{2+}-ATPase by electron microscopy of the two-dimensional Ca^{2+}-ATPase crystals induced by vanadate or lanthanides [1–3,64–67,69] revealed specific contacts between distinct surface regions of the ATPase molecules that give rise to the crystal lattice; these interactions were clearly different in the P2 type Ca^{2+}-ATPase crystals induced by vanadate that represent the E_2V conformation and in the P1 type crystals induced by lanthanides, that represent the E_1La conformation, indicating that they were influenced by the surface charge and/or conformation of the Ca^{2+}-ATPase.

The vanadate-induced Ca^{2+}-ATPase crystals consist of right-handed helical chains of Ca^{2+}-ATPase dimers (Figs. 5A and 6A) that are wound diagonally around the cylindrical sarcoplasmic reticulum at an angle of ≅ 57° to the long axis of the tubules [5]; the superimposition of the front and rear images of the flattened tubules creates a diamond-like pattern. The ATPase dimers are held together in an antiparallel arrangement by massive bridge-like structures, while the dimer chains are stabilized by interactions between the head and lobe regions of the pear-shaped ATPase contours above the surface of the bilayer [2,3].

Although the amino acid sequence of the Ca^{2+}-ATPase is known [6–8] and there are speculations about the probable folding of the polypeptide chain into structural and functional domains [9–11], the relationship of the ATPase contours revealed by crystallography to the primary sequence is entirely unknown.

We hoped that by analyzing the effect of monoclonal anti-ATPase antibodies of defined specificity on the stability of Ca^{2+}-ATPase crystals some information may be drawn about the relationship of the antigenic sites to the sites involved in the ATPase–ATPase interactions. Two types of experiments were performed. In experiments of one type the antibody solutions were preincubated with sarcoplasmic reticulum vesicles at 2°C, followed by centrifugation and resuspension in an antibody-free solution; the crystallization of the Ca^{2+}-ATPase was induced by the addition of 0.5 mM EGTA and 5 mM vanadate, and the effect of antibodies on the

Fig. 5. The effect of A52 antibody on the stability of Ca^{2+}-ATPase crystals. The crystallization of Ca^{2+}-ATPase was induced in sarcoplasmic reticulum vesicles (0.67–0.9 mg protein/ml) by incubation in a medium containing 0.1 M KCl, 10 mM imidazole (pH 7.4), 5 mM $MgCl_2$, 0.5 mM EGTA and 5 mM Na_3VO_4 at 2°C overnight. Aliquots were negatively stained with 1% uranyl acetate and viewed in a Siemens Elmiskop I electron microscope at 60 kV. (A) Control sarcoplasmic reticulum (0.9 mg protein/ml) after crystallization in the absence of antibodies. Magnification: 186000×. (B) Sarcoplasmic reticulum vesicles (0.9 mg protein/ml) crystallized as described above, but in the presence of 0.06 μg A52 antibody per μg sarcoplasmic reticulum protein. Magnification: 186000×. (C) Sarcoplasmic reticulum vesicles (0.67 mg protein/ml) treated as under A, but in the presence of 0.8 μg A52 antibody per μg sarcoplasmic reticulum protein. Magnification: 186000×.

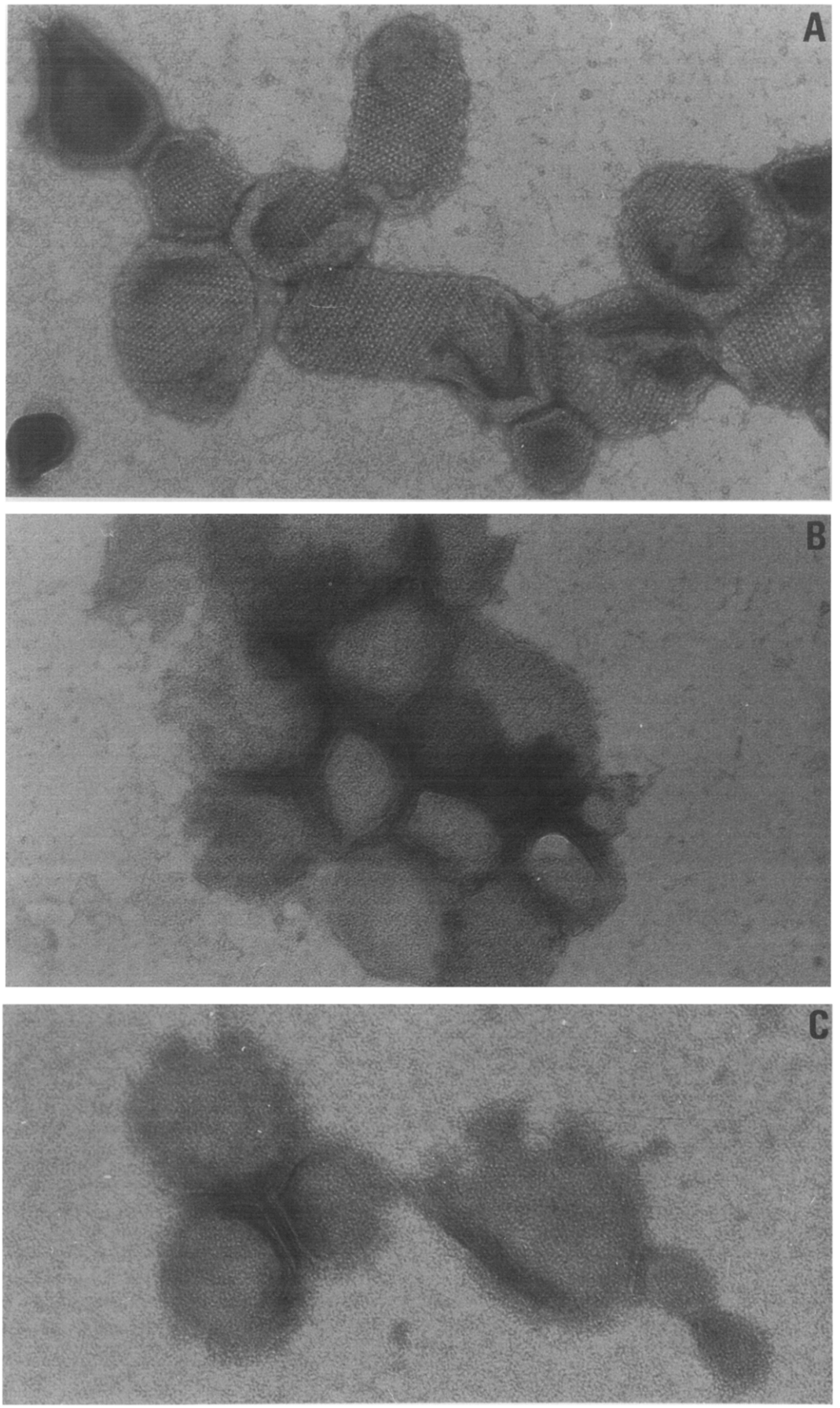
A
B
C

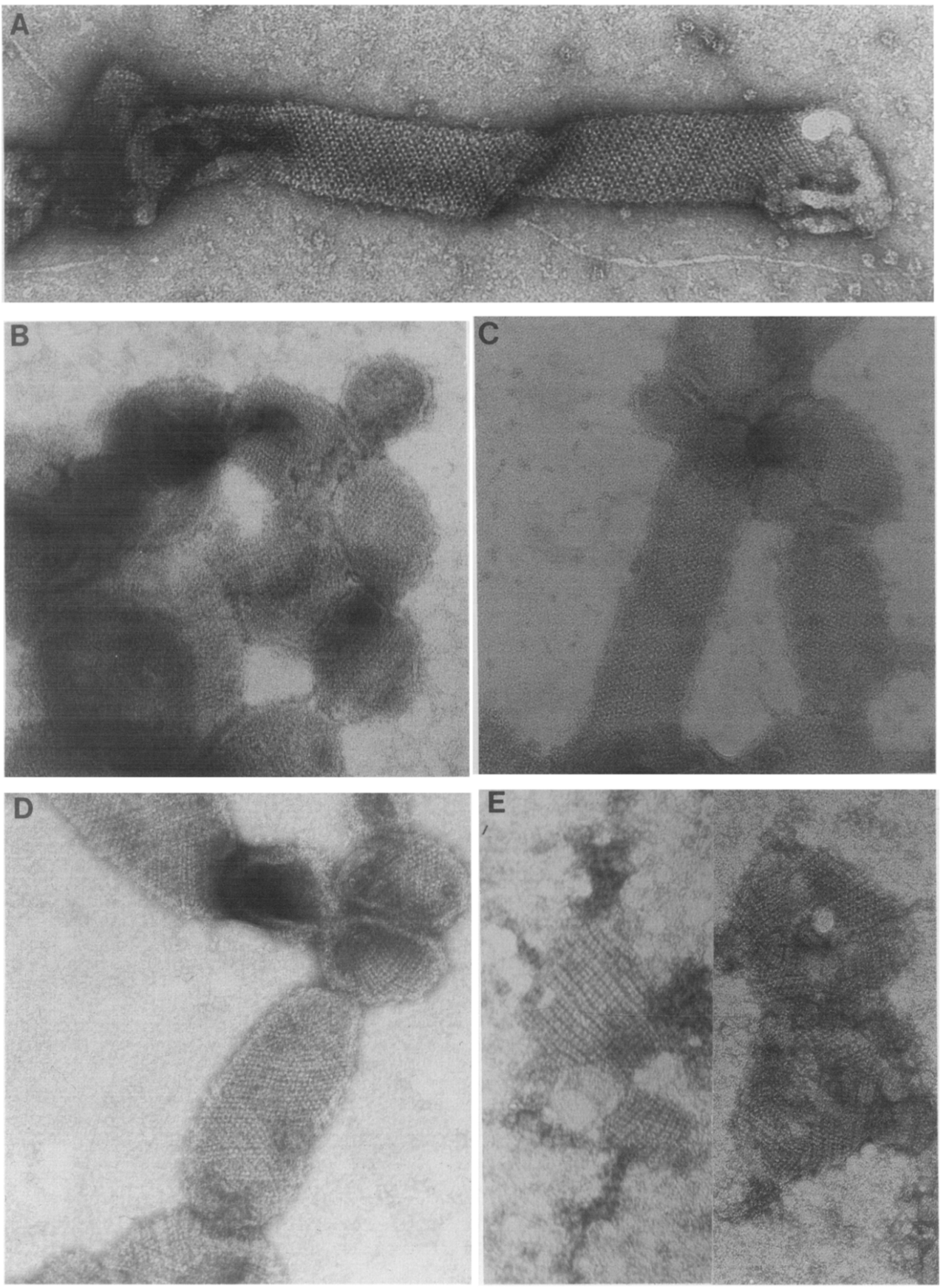
A
B
C
D
E

rate and extent of crystallization was followed as described earlier [65,71]. In experiments of the second type, Ca^{2+}-ATPase crystals were induced in sarcoplasmic reticulum vesicles by EGTA and vanadate in the absence of antibodies, and antibodies were introduced into the system after the crystals were fully developed.

Of the 19 antibodies that were screened, mAb A52 (Fig. 5), and pAb E (Fig. 6) were the most potent inhibitors of the crystallization of Ca^{2+}-ATPase induced by vanadate; A52 also decreased the stability of preformed Ca^{2+}-ATPase crystals (not shown). Three other monoclonal antibodies, $VE12_1G9$, 4B4 and D12, and one polyclonal antibody, N, also significantly interfered with crystallization (Fig. 6). All five antibodies have epitopes on the B tryptic fragment (Fig. 1), and all were found to react with the Ca^{2+}-ATPase in the native sarcoplasmic reticulum (Fig. 4, Table II).

Antibody A52 is particularly interesting, since its epitope is in a well defined region between residues 659 and 668, near Cys-670 and Cys-674, that serve as specific sites for reaction of Ca^{2+}-ATPase with IAEDANS [16,17]. The sequence of the A52 epitope is: Asp-Asp-Leu-Pro-Leu-Ala-Glu-Gln-Arg-Glu (MacLennan, D.H., personal communication).

The disordering of Ca^{2+}-ATPase crystals by mAb A52 begins at low A52 concentration (0.06 μg IgG/μg SR protein) by separation of the dimer chains from each other, producing disorganization of the lattice and the conversion of the elongated cylindrical tubules into spherical vesicles (Fig. 5B). At higher concentration of antibody (0.8 μg IgG/μg SR protein), the dimer chains completely disappear and aggregates of spherical vesicles with a random arrangement of surface particles form (Fig. 5C). The association of antibodies with the surface of the vesicles does not significantly increase the penetration of the negative stain into the vesicle interior, suggesting that the permeability properties of the membrane are not altered significantly. However, due to the binding of the antibody on the surface, the intermembrane space between aggregated vesicles increases from ≅ 100 Å in control sarcoplasmic reticulum (Fig. 5A), to ≅ 200 Å or more in sarcoplasmic reticulum treated with saturating concentration of A52 (Fig. 5C).

The amount of mAb A52 antibody bound to the sarcoplasmic reticulum was similar in the absence or presence of vanadate (Table II), indicating that the conformational change induced by vanadate did not alter the exposure of antigenic site or the affinity of the antibody toward the antigens. Therefore the affinity of A52 for its respective site on the Ca^{2+}-ATPase is sufficiently large to prevent the interaction between ATPase molecules that leads to crystallization in the absence of antibodies.

The binding of monoclonal and polyclonal antibodies to the Ca^{2+}-ATPase was similar whether they were added before or after the formation of extensive arrays of Ca^{2+}-ATPase crystals in the presence of vanadate (Table IV). Therefore the formation of the crystal lattice does not impose steric interference on the interaction of antibodies with their epitopes.

The simplest interpretation of the destabilization of Ca^{2+}-ATPase crystals by mAb A52 is that binding of the antibody to its antigenic site prevents the interaction between ATPase molecules by physical blocking of the surface where such interactions would take place. Considering the large bulk of the antibody, such interference is not unexpected, yet only few of the antibodies that bind to the Ca^{2+}-ATPase in the native sarcoplasmic reticulum produced disruption of the crystals, suggesting some degree of specificity in the effect. Further refinement of these experiments using Fab fragments will soon begin.

The polyclonal antibody E also completely prevented the formation of Ca^{2+}-ATPase crystals after incubation with sarcoplasmic reticulum at a concentration of 1.3 μg IgG/μg SR protein (Fig. 6B); under the same conditions incubation with control serum had no significant effect on crystallization (Fig. 6A). Some disorganization of the crystals was also observed after incubation with 0.8–1.2 μg 7C6 or $VE12_1G9$/μg SR protein (not shown).

Several antibodies altered in specific ways the pattern of crystallization without completely disrupting the crystal lattice. For example, the monoclonal antibody D12 caused marked separation of the dimer chains of Ca^{2+}-ATPase (Fig. 6D), suggesting that it interfered selectively with interaction between dimer chains that define their distance of separation within the lattice, but had no effect on the stability of ATPase dimers or their association into dimer chains. These observations suggest that D12 may be positioned between ATPase molecules in neighboring dimer chains. Similarly, monoclonal antibody 4B4 did not prevent crystallization, but

Fig. 6. The effect of antibodies on the crystallization of Ca^{2+}-ATPase in sarcoplasmic reticulum. Sarcoplasmic reticulum vesicles (0.5 mg/ml) were incubated in a medium of 0.1 M KCl, 10 mM imidazole (pH 7.4) and 5 mM $MgCl_2$ at 2°C for 1 h in the presence of control serum (A), 1.3 μg pAb E/μg SR protein (B), 0.75 μg 4B4/μg SR protein (C), 1 μg D12/μg SR protein (D), or anti-ATPase serum N at 1:5 dilution (E). After incubation the suspensions were diluted 100-fold with antibody-free medium, and centrifuged at 41000 × *g* for 40 min; the sedimented vesicles were suspended in an antibody-free crystallization medium containing 0.1 M KCl, 10 mM imidazole (pH 7.4), 5 mM $MgCl_2$, 0.5 mM EGTA and 5 mM vanadate to a protein concentration of 1 mg/ml and the crystallization was allowed to proceed for 24 h at 2°C. Samples were processed for electron microscopy as described in Methods. Magnification: 186000×.

TABLE IV

The binding of antibodies to the Ca^{2+}-ATPase before (column A) and after (column B) crystallization

A, antibodies added before crystallization. Antibody solutions diluted 1:5, 1:20 and 1:100 were preincubated at 2°C for 30 min with sarcoplasmic reticulum (0.67 mg protein/ml) or without sarcoplasmic reticulum, in a medium of 0.1 M KCl, 10 mM imidazole (pH 7.4) and 5 mM $MgCl_2$; after preincubation, 0.5 mM EGTA and 5 mM Na_3VO_4 were added and crystallization was allowed to proceed for 24 h at 2°C. The concentration of free antibody was determined after centrifugation at 10000 × *g* for 1 h by analysis of the supernatant with ELISA, using 1 μg sarcoplasmic reticulum protein fixed to the wells of the microtiter plates. Control antibody solutions were subjected to the same procedure except that sarcoplasmic reticulum was omitted during preincubation. The absorbance of the products of peroxidase reaction was measured at 405 nm. The difference in absorbance between the control samples and the samples obtained after preincubation with the sarcoplasmic reticulum was expressed as percent of the control absorbance. Column 1 identifies the code name of antibody. B, antibodies added after crystallization. To sarcoplasmic reticulum vesicles crystallized in a medium of 0.1 M KCl, 10 mM imidazole (pH 7.4), 5 mM $MgCl_2$, 0.5 mM EGTA and 5 mM Na_3VO_4 at 2°C for 24 h antibodies were added at 1:5, 1:20 and 1:100 dilution. After incubation for 24 h at 2°C the samples were centrifuged for 1 h at 10000 × *g* and the antibody content of the supernatant was measured, as described under A. The formation of crystals was tested by electron microscopy.

Antibody	Fraction of Ab bound to native sarcoplasmic reticulum (%)					
	1:5 dilution		1:20 dilution		1:100 dilution	
	A	B	A	B	A	B
A25	1	–	2	3	4	8
IIH11	0	–	0	–	4	–
7C6	9	4	38	39	76	76
8A6	0	0	0	0	17	10
11A4	0	6	0	0	0	0
A22	100 [a]	100 [a]	98	–	98	–
A52	1	0	84	94	79	91
$VE12_1G9$	0	–	7	–	40	–
VIE8	0	–	0	0	0	–
5D2	0	0	0	0	63	65
4B4	0	0	1	0	72	71
E	38	34	67	44	86	47
N	71	71	86	82	90	85
EM-1	41	–	78	–	85	–
EM-2 [b]	54	–	44	–	51	–
EM-3 [b]	18	–	37	–	40	–

[a] Note 1:2 dilution.
[b] Note 1:10, 1:30, 1:100 dilution.

the crystals lost their P2 symmetry; there were no clearly defined dimer chains (Fig. 6C) and the structure became reminiscent of the P1 crystals induced in sarcoplasmic reticulum by calcium or lanthanides [69,72]. After treatment of sarcoplasmic reticulum with the polyclonal antibody N, the normally observed vesicular structures were largely replaced by flat membrane sheets with clearly developed dimer chains of irregular disposition, that tend to fray around the edges of the membrane (Fig. 6E). These structures are reminiscent to osmotically lysed crystalline vesicles that are only rarely observed in preparations untreated by antibodies. Reconstruction of the structure of the Ca^{2+}-ATPase-antibody complexes from the electron micrographs of the modified crystalline arrays will permit a more precise assignment of the location of these antibodies on the ATPase molecule.

Monoclonal antibodies A22 and 5D2 and polyclonal antibodies EM-1, EM-2 and EM-3 had no discernible effect on the crystallization of Ca^{2+}-ATPase at a concentration of 1 μg/μg sarcoplasmic reticulum protein, although all these antibodies have epitopes in the exposed B region of the molecule and interacted with the Ca^{2+}-ATPase in the native sarcoplasmic reticulum membrane. All other antibodies were without effect, whether added before or after crystallization.

Antibody binding and the polarization of fluorescence of FITC covalently attached to the Ca^{2+}-ATPase

In detergent solutions of the Ca^{2+}-ATPase the polarization of fluorescence of FITC covalently attached to Lys-515 is near the theoretical limit ($P \cong 0.40$), indicating a rigid environment of the probe within the protein [73]. Interaction between ATPase molecules in the native membrane brings the fluorophores sufficiently close for energy transfer depolarization, and the polarization of fluorescence decreases to levels as low as $P = 0.2$ at high labeling ratios with FITC. Therefore the fluorescence polarization of FITC-labeled sarcoplasmic reticulum is a sensitive indicator of the state of association of ATPase molecules.

As shown in Table V, the polarization of fluorescence of FITC-Ca^{2+}-ATPase at a labeling ratio of ≅ 60–70% was $P = 0.32$–0.33 in the E_1 state stabilized by Ca^{2+} and increased to $P = 0.35$–0.37 in the E_2V state stabilized by vanadate and EGTA; this indicates some change either in the state of association or in the conformation of the Ca^{2+}-ATPase during transition between the E_1 and E_2V states. Small but significant increase in fluorescence polarization was observed upon the addition of the anti-B antibodies A52, $VE12_1G9$ and 5D2, both in the E_1 and E_2V states, and in the presence of 4B4 in the E_1 state. There was a slight decrease in polarization in the presence of VIE8 in the E_2V state (Table V). The effect with VIE8 was obtained at higher Ab/SR protein ratio than that used in the competitive binding assays (Fig. 4, Table II). The increase in fluorescence polarization is consistent with dissociation of ATPase oligomers [73], suggesting that antibodies A52, $VE12_1G9$, 5D2 and 4B4 interfere with ATPase–ATPase interactions. This class of antibodies is known to interact with the Ca^{2+}-ATPase in the native state (Table II), and A52, $VE12_1G9$, and 4B4 were also found to inhibit the formation of vanadate-induced E_2V type Ca^{2+}-

TABLE V

Polarization of fluorescence of FITC-Ca^{2+}-ATPase in the presence of various antibodies

Sarcoplasmic reticulum vesicles (50 μg protein/ml) were incubated at 10 °C in a medium of 0.1 M KCl, 10 mM imidazole (pH 7.4), 5 mM $MgCl_2$ and 0.1 mM $CaCl_2$ (E_1 state) or in a medium of 0.1 M KCl, 10 mM imidazole (pH 7.4), 5 mM $MgCl_2$, 1 mM EGTA and 5 mM Na_3VO_4 (E_2V state). Small aliquots of the various antibodies were added to the indicated final concentration and the polarization of fluorescence was measured at 525 nm, using light of 490 nm for excitation. The ΔP values represent the difference in polarization (P) between the antibody-containing samples, and their respective control samples. Monoclonal antibodies A25, IIH11, 7C6, 8A6, 11A4, A22, IID8, 5C3 and polyclonal antibodies E, N, EM-1, EM-2, EM-3 were also tested, but had no significant effect on the polarization of FITC fluorescence in either conformation.

Antibody code	Antibody concentration (μg Ab/μg SR)	Polarization (P)		ΔP	
		E_1	E_2V	E_1	E_2V
None (human serum)	–	0.319 ± 0.0006	0.352 ± 0.0007	−0.0007	0.0061
A52	1.50	0.326 ± 0.0008	0.366 ± 0.0007	0.0051	0.0071
$VE12_1G9$	12.00	0.336 ± 0.0005	0.387 ± 0.0005	0.0057	0.0183
VIE8	7.80	0.324 ± 0.0007	0.361 ± 0.0007	−0.0022	−0.0062
5D2	0.54	0.326 ± 0.0006	0.372 ± 0.0005	0.0070	0.0059
4B4	2.36	0.323 ± 0.0006	0.368 ± 0.0006	0.0061	0.0033

ATPase crystals (Figs. 5 and 6). These observations imply that the interactions involved in the stabilization of Ca^{2+}-ATPase oligomers in the noncrystalline sarcoplasmic reticulum [74,75] may also operate in the formation of the crystalline arrays of Ca^{2+}-ATPase.

The other antibodies were without effect on the

TABLE VI

The effect of antibodies on the Ca^{2+} transport and ATPase activity of sarcoplasmic reticulum

The effect of antibodies on oxalate-potentiated Ca^{2+} transport and Ca^{2+}-stimulated ATPase activity was determined as described under Methods. Sarcoplasmic reticulum vesicles were preincubated with various dilutions of the antiserum for 5–10 min at 20–24 °C, followed by measurement of the initial rate of Ca^{2+} transport and ATP hydrolysis, as described under Experimental Procedures. The Ca^{2+} capacity was defined as the amount of Ca^{2+} taken up by the sarcoplasmic reticulum after 5 min of incubation. The antibody/SR protein weight ratios are given in column 2, but tests were also carried out at lower and higher antibody concentrations. In each series of experiments several control samples were included without antibody or with non-immune serum. The % of control values refer to controls within each series. The data are presented as mean ± standard error, based on the number of independent measurements indicated in parentheses.

Antibody code	Antibody concn. (μg Ab prot./μg SR prot.)	Ca transport				ATPase activity	
		initial rate		Ca capacity			
		μmol Ca·mg^{-1}·min^{-1}	% of control	μmol Ca·mg^{-1}	% of control	μmol ATP·mg^{-1}·min^{-1}	% of control
A25	4.5	1.89 ± 0.22 (8)	83	5.01 ± 1.05 (2)	94	3.91 ± 0.64 (4)	105
IIH11	60.0	1.44 ± 0.14 (5)	65	3.27 ± 0.50 (2)	82	–	–
7C6	5.0	1.90 ± 0.13 (12)	99	4.28 ± 0.02 (3)	103	3.16 ± 0.15 (6)	108
8A6	5.0	1.94 ± 0.10 (12)	101	3.24 ± 0.05 (3)	83	3.03 ± 0.17 (6)	104
11A4	5.0	1.65 ± 0.16 (12)	86	4.32 ± 0.01 (3)	110	2.84 ± 0.10 (6)	97
A22	4.5	2.07 ± 0.24 (8)	90	5.49 ± 0.90 (2)	103	3.32 ± 0.08 (4)	89
A52	4.5	1.23 ± 0.10 (10)	54	4.13 ± 0.74 (2)	77	2.37 ± 0.13 (4)	64
$VE12_1G$	60.0	0.98 ± 0.09 (5)	44	3.15 ± 0.63 (2)	69	1.80 (1)	70
VIE8	40.0	2.05 ± 0.22 (5)	92	4.32 ± 0.69 (2)	94	–	–
5D2	5.0	1.20 ± 0.12 (12)	63	3.08 ± 0.12 (3)	74	2.20 ± 0.20 (7)	75
4B4	5.0	1.30 ± 0.12 (20)	70	4.14 ± 0.01 (3)	106	2.28 ± 0.21 (8)	79
D12	10.0	1.70 ± 0.05 (4)	68	3.98 ± 0.01 (2)	92	2.78 ± 0.11 (2)	89
E	25.0	1.46 ± 0.25 (12)	60	5.30 ± 0.74 (2)	99	1.97 ± 0.35 (6)	68
N	120.0 [a]	1.05 ± 0.17 (5)	74	1.17 ± 0.01 (2)	42	2.43 ± 0.21 (4)	81
EM-1	76.6 [a]	1.28 ± 0.12 (11)	90	2.51 ± 0.07 (5)	91	2.99 ± 0.14 (4)	100
EM-2	60.0 [a]	1.08 ± 0.08 (11)	76	2.56 ± 0.05 (5)	93	2.90 ± 0.23 (4)	97
EM-3	121.6 [a]	1.12 ± 0.08 (11)	79	2.36 ± 0.19 (5)	86	2.57 ± 0.18 (4)	86
IID8	46.0	1.75 ± 0.24 (5)	79	3.78 ± 0.70 (2)	82	–	–
5C3	5.0	1.67 ± 0.17 (6)	95	4.16 ± 0.03 (3)	100	3.00 ± 0.24 (3)	107

[a] For polyclonal antibodies N, EM-1, EM-2 and EM-3 the total antiserum protein concentration was used to calculate the data in column 2.

polarization of FITC fluorescence either in the E_1 or in the E_2V state (not shown).

ATPase activity and Ca^{2+} transport in the presence of Ca^{2+}-ATPase antibodies

The rate of ATP-dependent Ca^{2+} transport by the sarcoplasmic reticulum was inhibited by monoclonal antibodies A52, $VE12_1G9$, 5D2, 4B4 and D12 and by the purified polyclonal antibody E (Table VI); some inhibition of Ca^{2+} transport was also observed with IIH11 at very high antibody concentration. The inhibition of Ca^{2+} transport was accompanied by inhibition of ATPase activity, but the Ca^{2+} capacity of sarcoplasmic reticulum remained essentially unchanged by most of the antibodies, except pAb N, that significantly reduced Ca^{2+} capacity. In view of the unchanged Ca^{2+} capacity of the vesicles a change in Ca^{2+} permeability is not likely to play a role in the modest inhibition of Ca^{2+} transport by antibodies. The relatively slow rate of Ca^{2+} transport and ATP hydrolysis in the presence of antisera (pAb N, EM-1, EM-2, EM-3) may be in part due to inhibition by other serum components, since the values obtained with control sera were also lower than those of serum free controls.

The maximum inhibition of ATPase activity and Ca^{2+} transport by monoclonal antibodies was usually less than 50% and further increase in antibody concentration did not increase the inhibition. Under the conditions of these experiments the antigenic sites of the Ca^{2+}-ATPase were fully saturated by antibodies.

The rate of Ca^{2+} transport and ATP hydrolysis remained essentially unchanged by monoclonal antibodies 7C6 and A22, that clearly interact with the Ca^{2+}-ATPase. It was important to determine whether the binding of these antibodies to the enzyme was influenced by the conditions prevailing during Ca^{2+} transport. Neither ATP (10 mM) nor AMP-PNP (1 mM) had significant effect on the binding of mAb 7C6 and A22 to the Ca^{2+}-ATPase (Fig. 7); therefore, under the conditions of the ATPase assay antibodies 7C6 and A22 are likely to remain attached to the Ca^{2+}-ATPase. We conclude, in agreement with earlier observations [21,76], that the epitopes of antibodies 7C6 and A22 do not undergo large scale motions during ATP-dependent Ca^{2+} transport. Such motions would have been slowed by the attachment of the antibodies with decrease in Ca^{2+} transport rates and this was not observed.

The spatial relationship of antigenic sites to each other and to the attachment sites of fluorescent probes

The epitope for the A52 antibody on residues 659–668 is adjacent to the attachment sites for IAEDANS on Cys-670 and Cys-674 [16]. In view of this close proximity, the A52 binding site and the IAEDANS sites are likely to remain close neighbors in the folded native structure of the Ca^{2+}-ATPase. Lys-515 represents another well defined location that can be labeled selectively with fluorescein 5′-isothiocyanate. Based on fluorescence energy transfer, the distance between the covalently bound FITC and IAEDANS in the native enzyme is ≅ 58 Å [19], that is close to the largest dimension (≅ 60 Å) of the pear-shaped cytoplasmic domain seen in the reconstructed structure of the Ca^{2+}-ATPase [2,3].

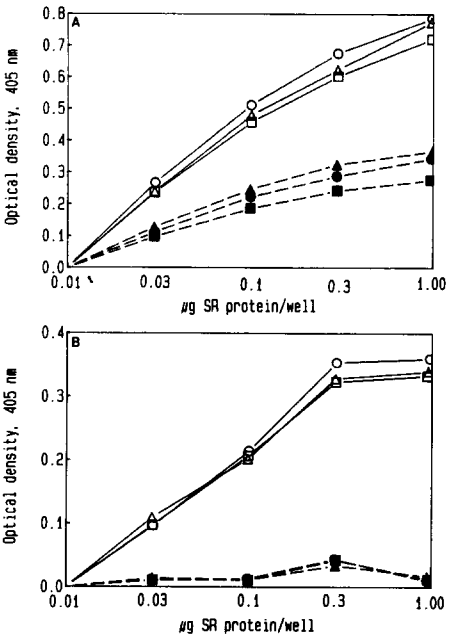

Fig. 7. Effect of ATP and AMP-PNP on the binding of 7C6 and A22 to the Ca^{2+}-ATPase. Sarcoplasmic reticulum vesicles (0.67 mg protein/ml) in 0.1 M KCl, 10 mM imidazole (pH 7.4), 5 mM $MgCl_2$, 0.1 mM $CaCl_2$ and either 10 mM ATP or 1 mM AMP-PNP or no nucleoside phosphate were incubated with mAb 7C6 (Fig. 7A) or A22 (Fig. 7B) at 1:100 dilution for 15 min and centrifuged at $10000 \times g$ for 1 h. The antibody content of the supernatant was assayed by ELISA at a final dilution of 1:1000, as described in Methods. Open symbols: preincubation without sarcoplasmic reticulum; filled symbols, preincubation with 0.67 mg SR protein/ml; ○, ●, no nucleoside phosphate; △, ▲, 10 mM ATP; □, ■, 1 mM AMP-PNP.

The spatial relationship of these two sites was further defined by testing the competition between antibodies directed against these two regions of the ATPase. Anti-FITC serum prepared in rabbits against FITC-labeled keyhole limpet hemocyanine reacted with the FITC-labeled Ca^{2+}-ATPase in native sarcoplasmic reticulum (Table VII). The polarization of fluorescence of FITC covalently bound to the Ca^{2+}-ATPase increased after binding of anti-FITC antibody from 0.3474 ± 0.0005 to 0.3522 ± 0.0004 in the presence of 0.1 mM $CaCl_2$ (E_1 state), and from 0.3513 ± 0.0007 to 0.3571 ± 0.0005 in the presence of 1 mM EGTA and 5 mM Na_3VO_4 (E_2V state). The binding of anti-FITC antibody did not influence the cleavage of the Ca^{2+}-ATPase at the nearby T_1 cleavage site between residues 505 and 506 (not shown).

TABLE VII

Competition between monoclonal antibodies and the polyclonal anti-FITC antibody for binding to FITC-labeled Ca^{2+}-ATPase in native sarcoplasmic reticulum

Sarcoplasmic reticulum vesicles were labeled with 5 nmol of FITC/mg protein, as described under Experimental Procedures. The binding of anti-FITC antibody to the native sarcoplasmic reticulum vesicles (0.67 mg protein/ml) was measured in a medium of 0.1 M KCl, 10 mM imidazole (pH 7.4), 5 mM $MgCl_2$, 0.5 mM EGTA and 5 mM Na_3VO_4 at 2°C; the anti-FITC serum was mixed with the vesicles at a final dilution of 1:100 in the absence or presence of monoclonal antibodies at 1:100 or 1:10 dilution, and incubated for 2 h followed by centrifugation at $10000 \times g$ for 1 h. Control samples were run under the same conditions without sarcoplasmic reticulum vesicles. The free anti-FITC antibody content of the supernatant was determined by ELISA at a further dilution of 1:10 (final dilution: 1:1000), using 0, 0.03, 0.1, 0.3 and 1 μg sarcoplasmic reticulum protein per well and an HRP conjugated goat anti-rabbit IgG for quantitation. Only data obtained with the highest concentration of sarcoplasmic reticulum protein (1 μg/well) are presented. The anti-rabbit IgG did not show cross-reaction with any of the mouse monoclonal antibodies used in these studies. The binding of anti-FITC antibody is expressed as percent of the antibody content obtained in the supernatant of control samples after preincubation of anti-FITC serum (1:100) in the same medium in the absence of sarcoplasmic reticulum. The binding of monoclonal antibodies A22, 7C6, 5D2, 4B4, D12 and A52 was also measured after preincubation at 1:100 and at 1:10 dilution, with or without sarcoplasmic reticulum, and with or without anti-FITC serum, under the same conditions described above. The last two columns of the table give the amount of monoclonal antibody bound as percent of the antibody content of the supernatant of control samples incubated without sarcoplasmic reticulum, either in the absence or in the presence of anti-FITC serum at 1:100 dilution. The monoclonal antibody concentration of the supernatants was measured by ELISA using HRP conjugated goat anti-mouse IgG for quantitation; the wells contained 0, 0.03, 0.1, 0.3 and 1.0 μg sarcoplasmic protein but only the data obtained at 1 μg/well are presented. There was no detectable cross-reaction between the anti-mouse IgG and the rabbit anti-FITC antibody.

Competing monoclonal antibody		Binding of anti-FITC antibody (1:100), percent		Binding of monoclonal antibody, percent	
code	dilution	−mAb	+mAb	−anti-FITC	+anti-FITC
None	–	54–66	–	–	–
A22	1:100	60	68	> 99	> 99
A22	1: 10	66	71	92	85
7C6	1:100	60	72	9	11
7C6	1: 10	66	81	17	12
5D2	1:100	60	65	69	70
5D2	1: 10	66	74	<1	<1
4B4	1:100	60	62	71	70
4B4	1: 10	66	76	4	1
D12	1: 10	66	65	64	51
A52	1:100	54	54	81	79
A52	1: 10	66	74	22	4

Based on quantitative ELISA, the interaction of the anti-FITC antibody with the FITC-labeled Ca^{2+}-ATPase was not affected by the saturation of the enzyme with the A52 antibody that binds at residues 659–668 in the vicinity of the IAEDANS sites or by the A22 antibody that has epitope on the B fragment in the region of residues 506–738 (Table VII). In view of the relatively small fractional binding of the A52 antibody at 1:10 dilution the difference between the percent binding values of A52 obtained in the presence and absence of anti-FITC serum is not considered significant. Therefore, in agreement with the fluorescence energy transfer data, the FITC binding site and the A52/IAEDANS region of the Ca^{2+}-ATPase are located sufficiently far apart on the ATPase molecule to permit simultaneous attachment of the two antibodies to their respective binding sites.

Similar competition experiments were also performed between the anti-FITC antibody and the monoclonal antibodies 5D2, 4B4 and D12 that bind to the native enzyme in the region corresponding to the B fragment, and the monoclonal antibody 7C6, that binds to the A_1 fragment. Neither of these antibodies showed significant competition with the binding of anti-FITC antibody or vice versa (Table VII).

Discussion

Until a high resolution structure of Ca^{2+}-ATPase becomes available the mapping of the functional sites on the enzyme must depend on the use of indirect approaches, such as site-specific fluorescent [19,77] or cross-linking reagents [75] and monoclonal antibodies [28,33,34,40,41,50].

There was considerable progress in recent years in the development of techniques that can be used to localize epitopes in various proteins [70], including the acetylcholine receptor [79], the Na^+/K^+-ATPase [80,81] and the Ca^{2+}-pump proteins of the plasma membranes of smooth muscle [44,82–84] and erythrocytes [85].

In this study we explored the effects of monoclonal and polyclonal antibodies on the ATPase–ATPase interactions in sarcoplasmic reticulum, with the aim of defining the regions on the surface of the Ca^{2+}-ATPase molecule, that are involved in protein-protein contacts in the native membrane and in the crystalline ATPase arrays induced by vanadate.

Of the 19 anti-ATPase antibodies tested, 12 interacted with the Ca^{2+}-ATPase in the native membrane and of these, four monoclonal antibodies (A52, $VE12_1G9$, D12 and 4B4) and two polyclonal antibodies (E and N) interfered with the crystallization of the Ca^{2+}-ATPase induced by vanadate.

The antibodies may inhibit crystallization by changing the conformation of the enzyme, by preventing the vanadate-induced conformational change that is required for crystallization, or by physically blocking the interaction between ATPase molecules.

The FITC covalently attached to the ATPase serves as a sensitive probe of the conformation of the protein, responding with a large change in fluorescence intensity

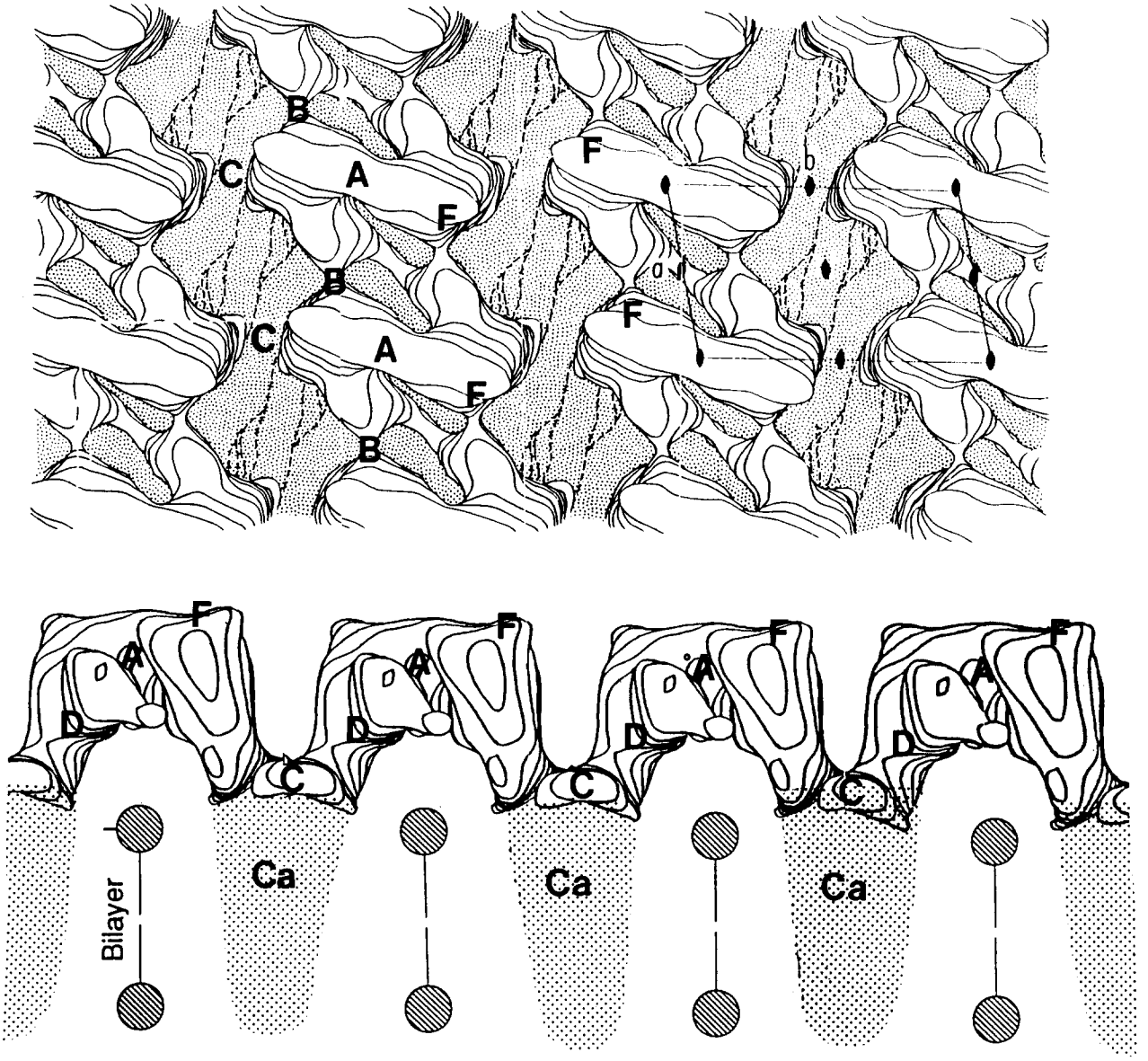

Fig. 8. Surface contours of the Ca^{2+}-ATPase. The surface contours of the Ca^{2+}-ATPase viewed normal to the membrane plane (top panel) and from within the membrane plane (bottom panel) are shown based on the data of Taylor et al. [2], obtained by electron microscope reconstructions of vanadate-induced E_2V type crystals. The unit cells indicated by lines 'a' and 'b' contains an ATPase dimer. The principal contact regions between the ATPase molecules in the lattice are marked by 'A', 'B', and 'C', as described in the text. The putative binding sites for FITC, AEDANS and Ca^{2+} are indicated by 'F', 'D' and 'Ca^{2+}', respectively. The binding site for mAb A52 is tentatively assigned to the 'D' region, while that for anti-FITC is tentatively assigned to the 'F' region.

during transition from the E_1 state stabilized by Ca^{2+} to the E_2V state stabilized by EGTA + vanadate [86–88]. The antibodies that disrupted the Ca^{2+}-ATPase crystals caused only slight change in the fluorescence intensity of FITC-Ca^{2+}-ATPase. Therefore we suggest that the inhibition of crystallization by A52, $VE12_1G9$, 4B4, D12, E and N is not caused by a change in enzyme conformation, but it is due to attachment of antibody to the Ca^{2+}-ATPase in a manner that physically blocks the ATPase–ATPase interactions required for crystallization.

There are several regions of contact between ATPase molecules in the crystalline arrays, that could be selectively affected by the antibodies (Fig. 8). The ATPase dimers are held together in an antiparallel arrangement by massive bridge-like structures above the surface of the bilayer (type A contact) [2,3]. These ATPase dimers are presumed to be the dominant form of the enzyme in native sarcoplasmic reticulum [75]. During vanadate-induced crystallization the ATPase dimers are linked into dimer chains by interactions between the head and lobe regions of ATPase molecules in the neighboring ATPase

dimers (type B contact) (Fig. 8). The crystalline arrays develop by interactions between the transmembrane segments of the neighboring dimer chains within the bilayer (type C contacts) that can be visualized by freeze-etch electron microscopy [89], or by electron microscopy of frozen-hydrated crystals [3,4].

The disruption of Ca^{2+}-ATPase dimer chains by mAb A52 was accompanied by an increase in the fluorescence polarization of FITC covalently bound to the Ca^{2+}-ATPase, consistent with the weakening of the type B contacts by mAb A52; this would prevent the formation of ATPase dimer-chains, without necessarily exerting a major effect on the concentration of the Ca^{2+}-ATPase dimers in the membrane. The increased separation of dimer chains and their less regular disposition with respect to the longitudinal axis of the tubules after treatment with antibodies D12 and N suggest interference with the type C interactions without major effect on the association of ATPase dimers into dimer chains. The conversion of the P2 into P1 type lattice after treatment with antibody 4B4 indicates a more subtle change in the relationship of the ATPase molecules, that cannot be defined by direct visual inspection of the electron micrographs, and requires three-dimensional reconstruction of the structure [4].

A possible arrangement of the functional sites, that is consistent both with the intramolecular distances determined by fluorescence energy transfer [19] and with the antibody binding data contained in this report, would position the binding site for IAEDANS (residue 670, 674) and for the A52 antibody (residues 659–668) near the tip of the lobe region, on the lower surface of the cytoplasmic mass close to the phospholipid headgroups, while the FITC binding site (Lys-515) would be located near the bridge on the head region at the opposite end of the molecule. The distance between these two sites is $\cong 60$ Å, consistent with the 58 Å distance calculated from energy transfer between covalently bound IAEDANS and FITC [19]. The assignment of the FITC site to the head region is also consistent with the estimated distance of 47 Å between the FITC site and the middle of the phospholipid bilayer, where the Ca^{2+} binding site is located [12]. The distance of the IAEDANS site to the Ca^{2+} binding site was estimated to be 16–18 Å [19], consistent with the location of this site closer to the cytoplasmic surface of the bilayer.

Positioning of the A52 binding site near the tip of the lobe would explain the disruption of Ca^{2+}-ATPase crystals by interference with the type B interactions; this could lead to the eventual dissociation of the dimer chains into randomly dispersed ATPase dimers, that may be still held together by the type A contacts near the middle of the bridge.

The lack of effect of antibodies A25, IIH11, 8A6 and 11A4 on the polarization of fluorescence of FITC-labeled Ca^{2+}-ATPase is not surprising, since these antibodies are not bound to the native Ca^{2+}-ATPase. Their antigenic sites may be located in the areas of the contacts between ATPase molecules that are not accessible for reaction in the native membrane. This would explain that the antigenic site of A25, 8A6 and 11A4 became exposed for reaction upon dissociation of ATPase oligomers into monomers in the presence of detergents.

Dissociation of oligomeric proteins at high pressure is well established [54]. Therefore the increased access of 8A6 and 11A4 to their binding sites during and after pressure treatment at 1.5 kbar for 2 h is also consistent with the location of their epitopes in the regions of interaction between ATPase molecules.

Of the antibodies that interact with the native Ca^{2+}-ATPase, $VE12_1G9$, A52, 4B4 and 5D2 caused small but significant increase in the polarization of fluorescence of FITC-Ca^{2+}-ATPase; we tentatively attribute this effect to dissociation of Ca^{2+}-ATPase tetramers into dimers or monomers by weakening of type A and B interactions. This interpretation is supported by the inhibition of the crystallization of Ca^{2+}-ATPase by A52, $VE12_1G9$ and 4B4. At low A52 concentration separation of dimer chains of Ca^{2+}-ATPase with disorganization of the lattice was observed that may indicate some direct or indirect effect of the antibody on the type C interactions as well.

The anti-FITC antibody did not influence the crystallization of Ca^{2+}-ATPase, presumably because the bound antibody was oriented in such a manner that it was not interposed between the ATPase molecules engaged in type A, B or C contacts.

The results of the competition experiments between various antibodies for binding sites on the Ca^{2+}-ATPase are consistent with the hypothesis outlined above. The binding of the anti-FITC antibody to FITC-labeled Ca^{2+}-ATPase was entirely unaffected by saturating concentration of the A52 antibody, that is assumed to bind at a considerable distance from the FITC binding site. The FITC and the IAEDANS sites are both located on the B fragment; therefore this region of the molecule appears to have a relatively open configuration extending over much of the cytoplasmic domain of the Ca^{2+}-ATPase. The ready access of nearly all anti-B antibodies to their binding sites and of trypsin to the T_1 cleavage sites in the native enzyme is consistent with this interpretation. There was also no effective competition between the anti-FITC antibody and monoclonal antibodies A22, 7C6, 5D2, 4B4 and D12.

The VIE8 antibody binds with moderate affinity to the Ca^{2+}-ATPase in the E_1 state stabilized by Ca^{2+}, but essentially no binding was observed in the E_2V state stabilized by EGTA and vanadate. The affinity of the epitope for VIE8 may be influenced by the conformational transition between the E_1 and E_2V states; alternatively the access to the binding site of VIE8 may be blocked in the E_2V conformation, either due to changes

in the secondary and tertiary structure of the Ca^{2+}-ATPase or due to interaction between ATPase molecules, that leads to crystallization in the E_2V state.

The polyclonal and monoclonal anti-Ca^{2+}-ATPase antibodies available to date have either no effect on the ATPase activity of sarcoplasmic reticulum or produce only partial inhibition, even at saturating concentrations [21,22,51,76]. A similar observation was made also on Na^+/K^+-ATPase [90]. The powerful inhibition of Ca^{2+} transport without inhibition of ATPase activity observed in earlier studies with some polyclonal anti-ATPase antibodies [91] was probably due to complement-dependent lesion of the membrane, that permitted the leakage of accumulated calcium [21]. The scarcity of inhibitory antibodies may imply that the active site of the Ca^{2+}-ATPase is either inaccessible or poorly antigenic, perhaps due to a unique secondary structure.

Colyer et al. [51] argued for a relationship between the inhibition of ATPase activity observed with some monoclonal antibodies and the location of their epitopes near the putative ATP binding and phosphorylation domain of the Ca^{2+}-ATPase. There is no direct evidence to support this assumption, and the incomplete inhibition of ATPase activity by monoclonal antibodies, even at saturating concentration argues against it. It is plausible to assume that the partial inhibition of ATPase activity and Ca^{2+} transport by monoclonal antibodies A52, $VE12_1G9$, 5D2, D12 and 4B4 may arise from interaction of antibodies with epitopes relatively distant from the active sites, provided the antibodies induce a structural change in the enzyme or interfere sterically with the traffic of substrates and the transitions in protein conformation required for Ca^{2+} transport. The inhibition observed with polyclonal antibodies may result from binding at several sites in view of their reaction with both the A and B regions of the Ca^{2+}-ATPase.

Some of the antibodies, notably A52, that inhibited ATP hydrolysis and Ca^{2+} transport also interfered with the crystallization of Ca^{2+}-ATPase and increased the fluorescence polarization of FITC-labeled Ca^{2+}-ATPase, suggesting an effect on ATPase–ATPase interactions. In view of the possible role of ATPase oligomers in ATP hydrolysis and Ca^{2+} transport [75], dissociation of naturally occurring ATPase dimers and tetramers by the antibodies may contribute to the changes in enzymatic activity. Therefore antibodies that interfere with ATPase–ATPase interactions may serve as probes for the exploration of the functional significance of ATPase oligomers in ATP hydrolysis and Ca^{2+} transport.

Acknowledgements

We wish to thank Drs. David H. MacLennan, Douglas M. Fambrough, Kevin P. Campbell and Angela F. Dulhunty for providing us with several of the antibodies used in these experiments. This study was supported by research grants from the NIH (AR 26545), the National Science Foundation (PCM 84-03679, Int. 86-17848) and the Muscular Dystrophy Association. The first two authors contributed equally to this study.

References

1 Taylor, K., Dux, L. and Martonosi, A. (1984) J. Mol. Biol. 174, 193–204.
2 Taylor, K.A., Dux, L. and Martonosi, A. (1986) J. Mol. Biol. 187, 417–427.
3 Taylor, K.A., Ho, M.-H. and Martonosi, A. (1986) Ann. NY Acad. Sci. 483, 31–43.
4 Taylor, K.A., Dux, L., Varga, S., Ting-Beall, H.P. and Martonosi, A. (1988) Meth. Enzymol. 157, 271–289.
5 Martonosi, A., Taylor, K.A., Varga, S. and Ting-Beall, H.P. (1987) in The Electron Microscopy of Proteins, Vol. 6, Membranous Structures (Harris, J.R. and Horne, R.W., eds.), pp. 255–376, Academic Press, New York.
6 MacLennan, D.H., Brandl, C.J., Korczak, B. and Green, N.M. (1985) Nature (London) 316, 696–700.
7 Brandl, C.J., Green, N.M., Korczak, B. and MacLennan, D.H. (1986) Cell 44, 597–607.
8 Brandl, C.J., DeLeon, S., Martin, D.R. and MacLennan, D.H. (1987) J. Biol. Chem. 262, 3768–3774.
9 Green, N.M., Taylor, W.R., Brandl, C., Korczak, B. and MacLennan, D.H. (1986) in Calcium and the Cell, CIBA Fnd. Symp. 122, pp. 93–113.
10 Green, N.M., Taylor, W.R. and MacLennan, D.H. (1988) in The Ion Pumps. Structure, Function, Regulation (Stein, W.D., ed.), pp. 15–24, Alan R. Liss, New York.
11 Taylor, W.R. and Green, N.M. (1989) Eur. J. Biochem. 179, 241–248.
12 Scott, T.L. (1985) J. Biol. Chem. 260, 14421–14423.
13 Scott, T.L. (1988) Mol. Cell. Biochem. 82, 51–54.
14 Clarke, D.M., Maruyama, K., Loo, T.W., Leberer, E., Inesi, G. and MacLennan, D.H. (1989) J. Biol. Chem. 264, 11246–11251.
15 Clarke, D.M., Loo, T.W., Inesi, G. and MacLennan, D.H. (1989) Nature 339, 476–478.
16 Kawakita, M. and Yamashita, T. (1987) J. Biochem. (Tokyo) 102, 103–109.
17 Bishop, J.E., Squier, T.C., Bigelow, D.J. and Inesi, G. (1988) Biochemistry 27, 5233–5240.
18 Mitchinson, C., Wilderspin, A.F., Trinnaman, B.J. and Green, N.M. (1982) FEBS Lett. 146, 87–92.
19 Squier, T.C., Bigelow, D.J., De Ancos, J.G. and Inesi, G. (1987) J. Biol. Chem. 262, 4748–4754.
20 Pick, U. and Bassilian, S. (1981) FEBS Lett. 123, 127–130.
21 Martonosi, A. and Fortier, F. (1974) Biochem. Biophys. Res. Commun. 60, 382–389.
22 Martonosi, A. (1975) in Calcium Transport in Contraction and Secretion (Carafoli, E., Clementi, F., Drabikowski, W. and Margreth, A., eds.), pp. 313–327, North-Holland Publ. Co., Amsterdam.
23 Hardwicke, P.M.D. (1976) Biochim. Biophys. Acta 422, 357–364.
24 Holland, P.C. and MacLennan, D.H. (1976) J. Biol. Chem. 251, 2030–2036.
25 Stewart, P.S., MacLennan, D.H. and Shamoo, A.E. (1976) J. Biol. Chem. 251, 712–719.
26 Jørgensen, A.O., Kalnins, V. and MacLennan, D.H. (1979) J. Cell Biol. 80, 372–384.
27 Jørgensen, A.O., Shen, A.C.Y., MacLennan, D.H. and Tokuyasu, K.T. (1982) J. Cell Biol. 92, 409–416.

28 Jørgensen, A.O., Arnold, W., Pepper, D.R., Kahl, S.D., Mandel, F. and Campbell, K.P. (1988) Cell Motil. Cytoskel. 9, 164–174.
29 DeFoor, P.H., Levitsky, D., Biryukova, T. and Fleischer, S. (1980) Arch. Biochem. Biophys. 200, 196–205.
30 Betto, R., Damiani, E., Biral, D. and Mussini, I. (1981) J. Immunol. Meth. 46, 289–298.
31 Damiani, E., Betto, R., Salvatori, S., Volpe, P., Salviati, G. and Margreth, A. (1981) Biochem. J. 197, 245–248.
32 Damiani, E., Margreth, A., Furlan, A., Dahms, A.S., Arnn, J. and Sabbadini, R.A. (1987) J. Cell Biol. 104, 461–472.
33 Zubrzycka-Gaarn, E., Phillips, L. and MacLennan, D.H. (1984) in Epithelial Calcium and Phosphate Transport: Molecular and Cellular Aspects (Bonner, F. and Peterlik, M., eds.), pp. 19–23, Alan R. Liss, New York.
34 Zubrzycka-Gaarn, E., MacDonald, G., Phillips, L., Jørgensen, A.O. and MacLennan, D.H. (1984) J. Bioenerg. Biomembr. 16, 441–464.
35 Jørgensen, A.O. and Campbell, K.P. (1986) Biophys. J. 49, 589a.
36 Pepper, D.R., Raab, C.R. and Campbell, K.P. (1986) Biophys. J. 49, 589a.
37 Leberer, E. and Pette, D. (1986) Eur. J. Biochem. 156, 489–496.
38 Levitsky, D.O., Syrbu, S.I., Cherepakhin, V.V. and Rokhlin, O.V. (1987) Eur. J. Biochem. 164, 477–484.
39 Levitsky, D.O., Syrbu, S.I., Cherepakhin, V.V. and Rokhlin, O.V. (1987) Biomed. Biochim. Acta 46, S382–S387.
40 Dulhunty, A.F., Banyard, M.R.C. and Medveczky, C.J. (1987) J. Membr. Biol. 99, 79–92.
41 Kaprielian, Z. and Fambrough, D.M. (1987) Dev. Biol. 124, 490–503.
42 Maier, A., Leberer, E. and Pette, D. (1988) Histochemistry 88, 273–276.
43 Sarkadi, B., Enyedi, A., Penniston, J.T., Verma, A.K., Dux, L., Molnar, E. and Gardos, G. (1988) Biochim. Biophys. Acta 939, 40–46.
44 Grover, A.K., Boonstra, I., Garfield, R.E. and Campbell, K.P. (1988) Biochem. Arch. 4, 169–179.
45 Krenacs, T., Molnar, E., Dobo, E. and Dux, L. (1989) Histochem. J. 21, 145–155.
46 Matthews, I., Colyer, J., Mata, A.M., Lee, A.G., Green, N.M. and East, J.M. (1989) Biochem. Soc. Trans. 17, 708–709.
47 Ohlendieck, K. and Ryan, N.M. (1989) Biochem. Soc. Trans. 17, 671–673.
48 Mata, A.M., Lee, A.G. and East, J.M. (1989) FEBS Lett. 253, 273–275.
49 Wuytack, F., Kanmura, Y., Eggermont, J.A., Raeymaekers, L., Verbist, J., Hartweg, D., Gietzen, K. and Casteels, R. (1989) Biochem. J. 257, 117–123.
50 Karin, N.J., Kaprielian, Z. and Fambrough, D.M. (1989) Mol. Cell. Biol. 9, 1978–1986.
51 Colyer, J., Mata, A.M., Lee, A.G. and East, J.M. (1989) Biochem. J. 262, 439–447.
52 Boland, R., Martonosi, A. and Tillack, T.W. (1974) J. Biol. Chem. 249, 612–623.
53 Nakamura, H., Jilka, R.L., Boland, R. and Martonosi, A.N. (1976) J. Biol. Chem. 251, 5414–5423.
54 Varga, S., Mullner, N., Pikula, S., Papp, S., Varga, K. and Martonosi, A. (1986) J. Biol. Chem. 261, 13943–13956.
55 Lowry, O.H., Rosebrough, N.J., Farr, A.L. and Randall, R.J. (1951) J. Biol. Chem. 193, 265–276.
56 Dean, W.L. and Tanford, C. (1977) J. Biol. Chem. 252, 3551–3553.
57 Martonosi, A. and Feretos, R. (1964) J. Biol. Chem. 239, 648–658.
58 MacLennan, D.H. (1970) J. Biol. Chem. 245, 4508–4518.
59 Goding, J.W. (1986) Monoclonal Antibodies: Principles and Practice. Production and Application of Monoclonal Antibodies in Cell Biology, Biochemistry and Immunology, 2nd End., Academic Press, New York.
60 Dux, L., Papp, S. and Martonosi, A. (1985) J. Biol. Chem. 260, 13454–13458.
61 Laemmli, U.K. (1970) Nature 227, 680–685
62 Johnson, D.A., Gautsch, J.W., Sportsmann, J.R. and Elder, J.H. (1984) Gene Anal. Techn. 1, 3–8.
63 Sargent, M.G. (1987) Anal. Biochem. 163, 476–481.
64 Dux, L. and Martonosi, A. (1983) J. Biol. Chem. 258, 2599–2603.
65 Dux, L. and Martonosi, A. (1983) J. Biol. Chem. 258, 10111–10115.
66 Dux, L. and Martonosi, A.N. (1983) J. Biol. Chem. 258, 11896–11902.
67 Dux, L. and Martonosi, A.N. (1983) J. Biol. Chem. 258, 11903–11907.
68 Michalak, M. (1985) in The Enzymes of Biological Membranes, 2nd Edn. Vol. 3 (Martonosi, A., ed.), pp. 115–155, Plenum Press, New York.
69 Dux, L., Taylor, K.A., Ting-Beall, H.P. and Martonosi, A. (1985) J. Biol. Chem. 260, 11730–11743.
70 Van Regenmortel, M.H.V. (1989) Immunol. Today 10, 266–272.
71 Dux, L. and Martonosi, A. (1984) Eur. J. Biochem. 141, 43–49.
72 Dux, L., Pikula, S., Mullner, N. and Martonosi, A.N. (1987) J. Biol. Chem. 262, 6439–6442.
73 Highsmith, S. and Cohen, J.A. (1987) Biochemistry 26, 154–161.
74 Papp, S., Pikula, S. and Martonosi, A. (1987) Biophys. J. 51, 205–220.
75 Keresztes, T., Jona, I., Pikula, S., Vegh, M., Mullner, N., Papp, S. and Martonosi, A. (1989) Biochim. Biophys. Acta 984, 326–338.
76 Dutton, A., Rees, E.D. and Singer, S.J. (1976) Proc. Natl. Acad. Sci. USA 73, 1532–1536.
77 Jona, I., Matko, J. and Martonosi, A. (1990) Biochim. Biophys. Acta, submitted.
78 McIntosh, D.B. and Ross, D.C. (1985) Biochemistry 24, 1244–1251.
79 Tzartos, S.J., Kordossi, A., Walgrave, S.L., Kokla, A. and Conti-Tronconi, B.M. (1988) Monogr. Allergy 25, 20–32.
80 Felsenfeld, D.P. and Sweadner, K.J. (1988) J. Biol. Chem. 263, 10932–10942.
81 Satoh, K., Nakao, T., Nagai, F., Kano, I., Nakagawa, A., Ushiyama, K., Urayama, O., Hara, Y. and Nakao, M. (1989) Biochim. Biophys. Acta 994, 104–113.
82 Wuytack, F., De Shutter, G., Verbist, J. and Casteels, R. (1983) FEBS Lett. 154, 191–195.
83 Verbist, J., Wuytack, F., Raeymaekers, L. and Casteels, R. (1985) Biochem. J. 231, 737–742.
84 Grover, A.K. (1988) J. Biol. Chem. 263, 19510–19512.
85 Caride, A.J., Gorski, J.P. and Penniston, J.T. (1988) Biochem. J. 255, 663–670.
86 Pick, U. (1982) J. Biol. Chem. 257, 6111–6119.
87 Pick, U. and Karlish, S.J.D. (1982) J. Biol. Chem. 257, 6120–6126.
88 Jona, I. and Martonosi, A. (1986) Biochem. J. 234, 363–371.
89 Ting-Beall, H.P., Burgess, F.M., Dux, L. and Martonosi, A. (1987) J. Musc. Res. Cell. Motil. 8, 252–259.
90 Ball, W.J., Schwartz, A. and Lescard, J.L. (1986) Biochemistry 25, 7155–7162.
91 Sumida, M. and Sasaki, S. (1975) J. Biochem. (Tokyo) 78, 757–762.